Project No. 01-59

PROPOSED ENHANCEMENTS TO PAVEMENT ME DESIGN: IMPROVED CONSIDERATION OF THE INFLUENCE OF SUBGRADE SOILS SUSCEPTIBLE TO FROST HEAVE ON PAVEMENT PERFORMANCE

APPENDIX 13

DEVELOPMENT AND CALIBRATION OF NEW EMPIRICAL MODEL FOR PAVEMENT SUBJECTED TO EFFECTS OF FROST HEAVE ON IRI

MAY 2023

TABLE OF CONTENTS

LIST OF FIGURES

LIST OF TABLES

13. DEVELOPMENT AND CALIBRATION OF NEW EMPIRICAL MODEL FOR PAVEMENT SUBJECTED TO EFFECTS OF FROST HEAVE ON IRI

13.1 Introduction

This Appendix discusses a new IRI prediction model for pavements subjected to frost heave. The model considers various environmental factors affecting IRI. The work reported in this appendix is a supplement work about IRI model calibration. It has nothing to do with the simplified 1-D model discussed in Appendix 6 and 7. Neither the 1-D model coded user interface nor the Monte Carlo analysis based IRI model calibration were related to the empirical model pretend in this Appendix. The empirical model was proposed by considering the physical process of frost have and pavement interactions. The site monitored IRI, distress data, and different site factors were used for the empirical model regression and calibration.

13.2 Objectives

The following objectives were completed as part of this study:

1. Observe the general trend of IRI variation with time for frost susceptible sections
2. Propose the new IRI prediction models based on the observed trend of IRI vs. time
3. Calibrate the new IRI prediction models for flexible pavement, rigid pavement, and HMA overlay pavement respectively.
4. Present one calculation example to show how to apply the new empirical model to predict IRI variation with time.
5. Discuss the inputs of the three design levels of the proposed empirical models

13.3 Relative background

The team did lots of work on LTPP data collection and re-organization, during which it is found that the complied data is not only appliable for the 1-D model calibration but also appliable for proposing independent empirical IRI estimation models. Hence, the empirical IRI models were first developed based on the physical principles. Then, the developed models were calibrated via the collected LTPP data. Through regression trials, it is found that the temperature, precipitation, and soil gradation can influence the frost heave induced IRI. These factors were related to the coefficients of the empirical IRI equations. Considering different mechanical characteristics of surface type, distinct empirical equations were proposed and calibrated for flexible pavement, rigid pavement and HMA overlay pavement separately.

13.4 The new IRI model for flexible pavement

13.4.1 IRI variation with time of sections suffering frost heave

From the processed LTPP database as discussed in Appendix 12, 158 sets of data of flexible pavement (located in 6 states and 8 sections) were selected specifically to observe the general trends of IRI variations with time. The observation of the IRI variation trend gives hints on the development of the new empirical IRI prediction equations. The 158 sets of data were selected based on below criteria:

1) Sections that are very likely to experience frost heave: the minimum FD (evaluated by Yoder and Witczak 1975 using annual FI) is larger than the thickness above the subgrade;

Minimum annual accumulated precipitation is larger than 1 ft (to represent enough water supply); soil particle gradation that includes at least 10% fine content and more than 10% silt content (except one section: Vermont 1002) to ensure the frost susceptibility.

2) The selected sections must possess available data of site measured initial IRI.
3) The selected sections much have at least 3 adjacent data points with time gap not larger than 1 year (or at least three IRI data within one year). It is noted that some frost susceptible sections have available data satisfying criteria 2, but the gap in the dates of data collection is larger than 1 year. These data were not used in the data analyses.
4) To avoid the influence of maintenance, only data within a single construction duration (no maintenance activities during the period) are used for analyses.
5) The selected sections have wPI<10, which is to exclude the influence of the expansive soil

Due to the above criteria constraints, relatively limited data sets were obtained for analyses. The details of the selected section are shown in Table 13- 1 below.

Table 13- 1 Summary of 8 road sections subjected to frost effects from LTTP

STATE _CODE	SHRP_ID	Min annual FI (deg F deg days)	Min FD (ft) by Yoder and Witczak 1975	Min annual precip.(in)	Subgrade: average of SILT %	Subgrade: average of CLAY%	Maintenance history	Thickness above subgrade (ft)	Available data sets
9	1803	>400	>1.64	>48	47.15	7.15	Yes	1.57	6
23	1026	>1500	>4.27	>48	10.15	1.75	Yes	0.69	9
23	1026	>1500	>3.94	>33	10.15	1.75	Yes	2.23	8
30	8129	>700	>2.46	>15	35.85	21.90	Yes	2.17	14
36	0801	>200	>1.64	>30	22.70	6.23	No	1.18	29
36	0802	>200	>1.64	>30	16.4	5.5	Yes	1.57	18
36	0859	>200	>1.64	>30	12.4	4.9	Yes	1.57	20
50	1002	>1100	>3.61	>33	4.30	2.60	No	2.85	36
83	1801	>2500	>5.81	>17	11.80	7.90	Yes	1.94	8
83	1801	>2400	>5.74	>15	11.80	7.90	Yes	1.94	10

As shown in the Table 13- 1, most of the sections have fine-grained subgrade soil, except for the sections 23-1026 and 50-1002. Most of the sections have maintenance history, except 36-0801 and 50-1002. Some of the sections in the table have more than one set of data (e.g., 23-1026, and 83-1801) but with different construction numbers. To minimize the maintenance effect, the SF-attenuation method (see definition in Appendix 12) was used. Note that the thickness of pavement structure above the subgrade may be changed due to maintenance. For example, for section 23-1006 in the Table, the second sets of data are recorded after adding an asphalt concrete overlay, hence, the thickness is increased.

To determine the proper mathematical formation of the new IRI model for flexible pavement, the general IRI vs. pavement age trend was observed. Ten typical pavement sections subjected to frost heave were selected for the observation. The study used data of the 9 sections collected and processed from LTPP, which is well discussed in Appendix 12. The plots of site measured IRI vs. age of the 9 sections are presented in Figure 13- 1 to Figure 13- 6. In these figures, the integer number of age represents the start of one year (January 1st). All site-measured data is represented by the dots instead of continuous curves. This is because the time gaps between any two points are usually different. The continuous curve may not be able to describe the true IRI variation trend between two points with relatively large time gaps. According to the plots in Figure 13- 1 to Figure 13- 6, the general features of IRI variations in different seasons can be found. During the non-freezing-thawing season, the IRI generally increased with time. The power regression ($IRI = a * t^b$) of each set of data were also shown in these figures. The regressed power terms of most sections

are less than 1, which indicates a slowly increased site-IRI with time for flexible pavements. For most sections, after freezing season begins, the IRI starts to increase aggressively. During the freezing-thawing season (March to May), the increased IRI values usually go to a peak, and as a result, a curve jump can be observed during this time. The apparently increased IRI is believed to be caused by the accumulated frost heave and material strength lost due to thaw weakening. The cumulative frost heave is closely correlated with the cumulative freezing index during the freezing season. After the freezing-thawing season, the IRI slightly decreases and then starts to increase again when the next freezing season starts.

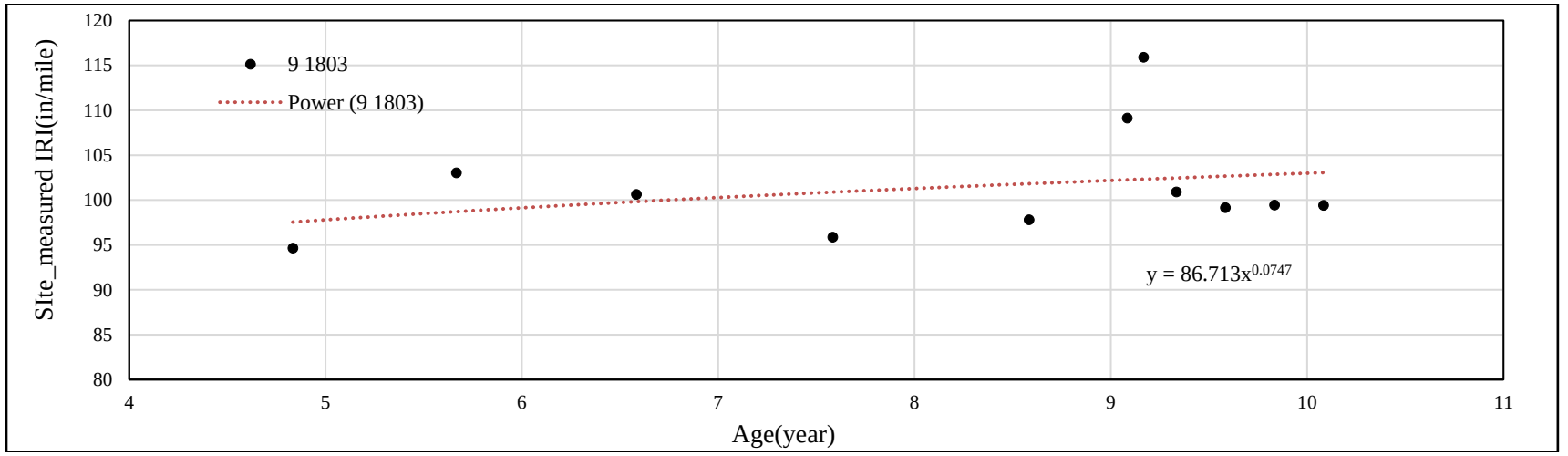

Figure 13- 1 Section 09-8013: site-measured IRI varied with time (pavement age from construction)

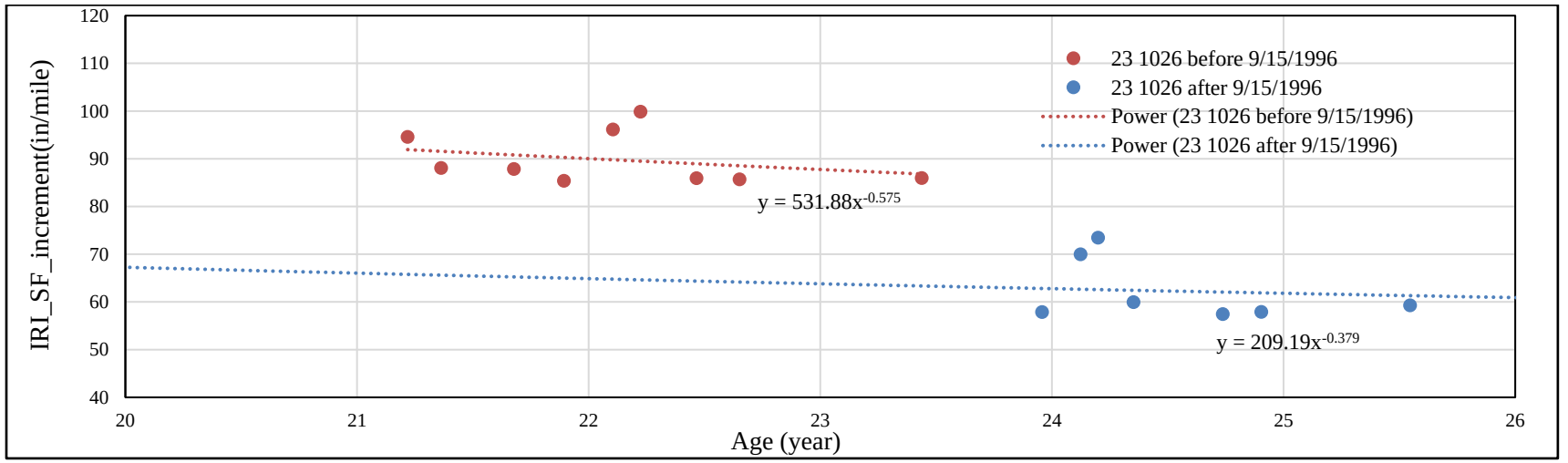

Figure 13- 2 Sections of state #23: site-measured IRI varied with time (pavement age from construction)

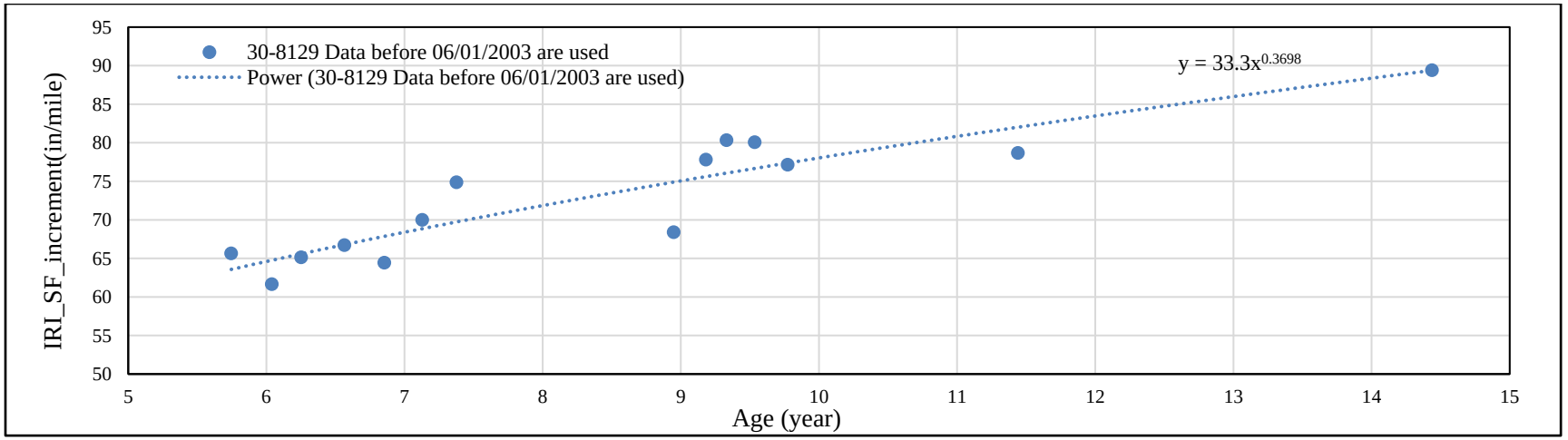

Figure 13- 3 Sections 30-8129: site-measured IRI varied with time (pavement age from construction)

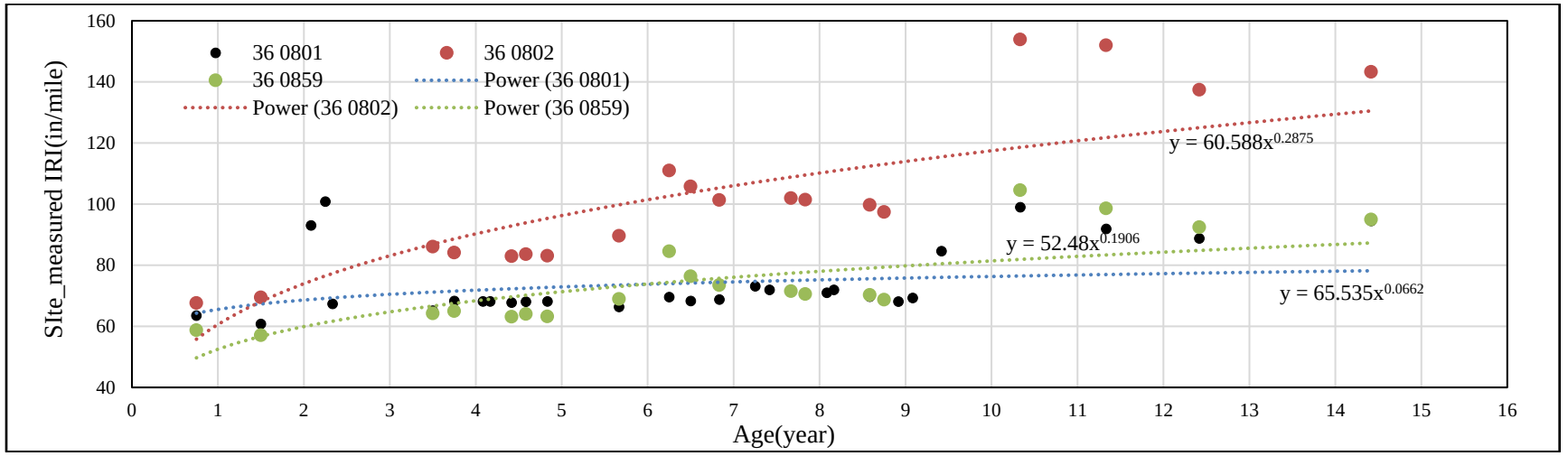

Figure 13- 4 Sections of state #36: site-measured IRI varied with time (pavement age from construction)

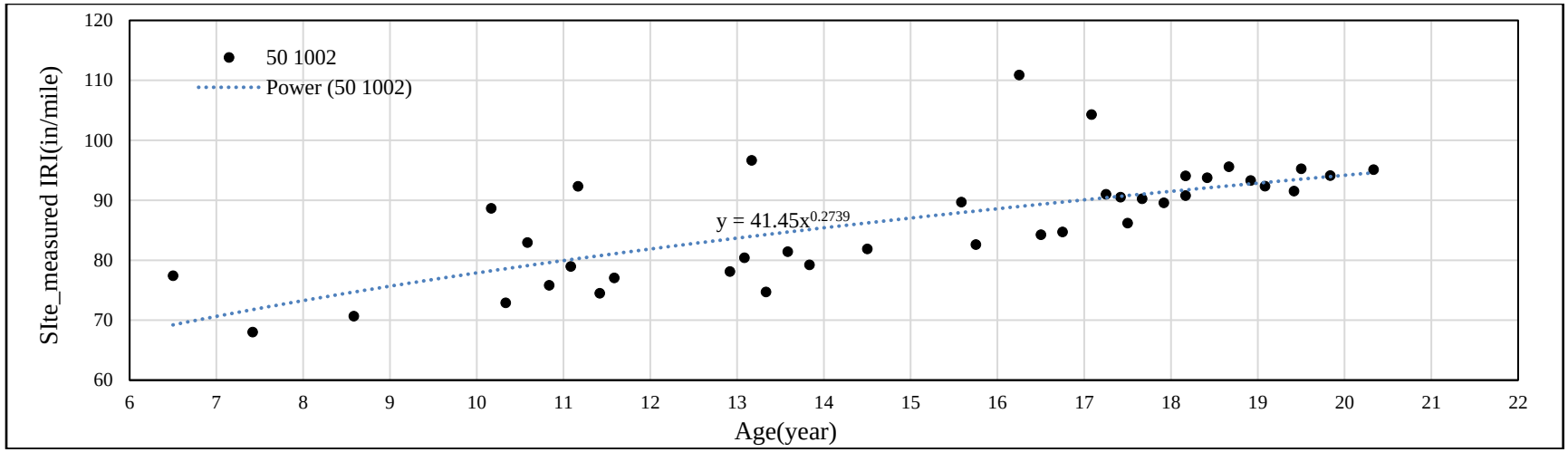

Figure 13- 5 Sections 50-1002: site-measured IRI varied with time (pavement age from construction)

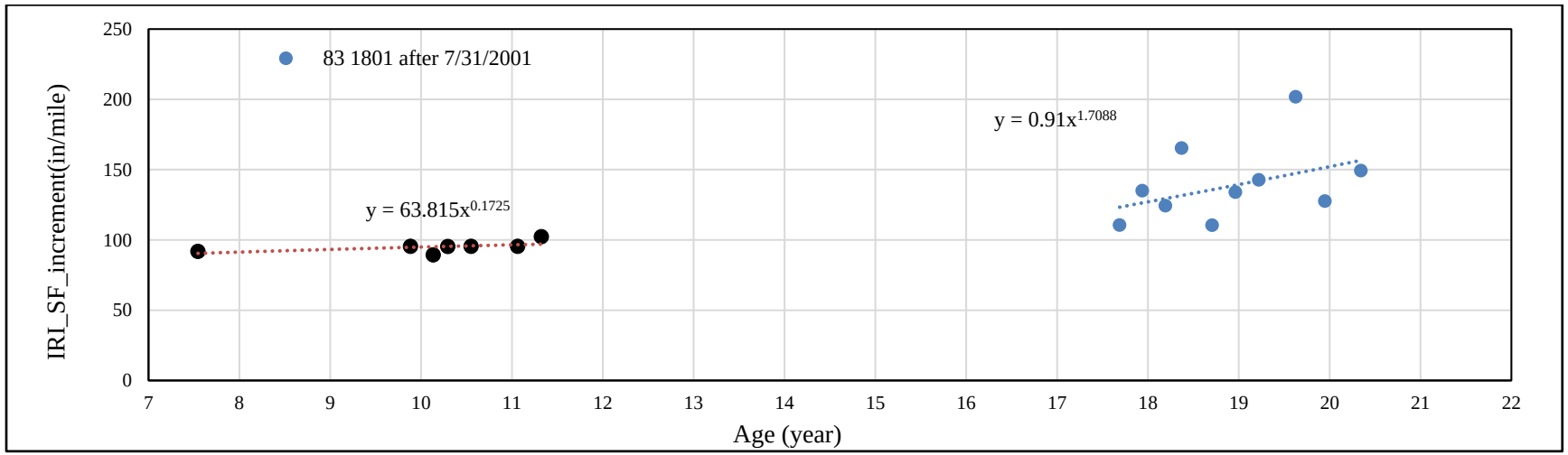

Figure 13- 6 Sections 93-1801: site-measured IRI varied with time (pavement age from construction)

13.4.2 New IRI model to site factor conditions due to frost heave

The MEPDG IRI model expression (2020 version) is shown below:

$$IRI = IRI_0 + IRI_{SF} + c_1(FC_{Total}) + c_2(TC) + c_3(RD) \quad \textbf{(13- 1)}$$

where c_1, c_2, and c_3 are calibration coefficients of pavement distress terms; IRI_0 is the initial IRI; IRI_{SF} is the IRI increment caused by site factors (including the pavement age). The way to consider IRI_0 and age are well discussed in Appendix 12, which is also used for the following empirical models calculaions. IRI_{SF} is believed to be related with frost and thawing influence. Even though it is impossible to directly measure IRI_{sf} on site, according to IRI_{sf} definition, the theoretical site-monitored IRI_{sf} can be estimated through subtracting the other measured terms from the measured IRI in equation (13- 1). In the following discussion, all the field IRI_{sf} is evaluated via such back calculation method and hereafter denotes as the site-measured IRI_{sf}. Based on the general observation of the IRI variation trend as discussed in 13.4.1, a new calibration equation for IRI_{SF} is proposed:

$$\mathrm{IRI_{sf}} = \mathrm{IRI_{sf_{ref}}} * [\mathrm{age}^{\mathrm{beta}} + \mathrm{gama} * \mathrm{FI_{accum}} * \sin(2\pi * \mathrm{month}/12 + \mathrm{eta})] \quad \textbf{(13- 2)}$$

In Equation (13- 2), the $\mathrm{IRI_{sf}}$ is attributed to three major components: 1) $\mathrm{IRI_{sf_{ref}}}$: it considers how the subgrade soil properties react with pavement structure and then affects the pavement surface; 2) $\mathrm{age}^{\mathrm{beta}}$: it describes the overall growth of IRI over time due to continued degradation of pavement subject to climate; 3) $\mathrm{gama} * \mathrm{FI_{accum}} * \sin(2\pi * \mathrm{month}/12 + \mathrm{eta})]$: it controls the contributions of freezing/thawing seasons.

The parameter $\mathrm{IRI_{sf_{ref}}}$ is described by the following relationship, which is validated with LTTP data later:

$$\mathrm{IRI}_{sf_{ref}} = \mathrm{IRI_{sf_{max}}} * DF_T \quad \textbf{(13- 3)}$$

where $\mathrm{IRI_{sf_{max}}}$ is the pure ground (no pavement structure) IRI increment caused by site factors and DF_T is the deduction factor of thickness that describes the thickness impact on the $\mathrm{IRI_{sf_{max}}}$. More specifically, $\mathrm{IRI_{sf_{max}}}$is the conceptual IRI of subgrade soil due to site factors which is related to the effects of FI, properties of subgrade soil and precipitation. If the pavement structure has no stiffness, the $\mathrm{IRI_{sf_{max}}}$ will propagate to the pavement surface without any change. However, in real situations, the pavement stiffness affects the propagation of $\mathrm{IRI_{sf_{max}}}$ and usually has impaired IRI on pavement surface. When the structure thickness increases to a certain extreme value, it will be too strong to have the $\mathrm{IRI_{sf_{max}}}$transmit to structure top, and therefore cannot cause additional site factor caused IRI. Eq.(2-5) captures these physics phenomena.

The term $\mathrm{age}^{\mathrm{beta}}$ describes the power law trend of IRI vs. time ($IRI = a * t^b$).Via numerical regression trials, it is found that beta is a factor related to pavement structural design (type of pavement and thickness of pavement structure), which controls the general age-dependent IRI increment trend with time.

In the term $\mathrm{gamma} * \mathrm{FI_{accum}} * \sin(2\pi * \mathrm{month}/12 + \mathrm{eta})$, gamma is the factor that controls the magnitude of frost or thaw related IRI fluctuation; $\mathrm{FI_{accum}}$ is the monthly freezing index accumulated from the start of freezing season of last year to the beginning of the non-freezing season of next year; eta is a factor that governs the sine wave phase position of IRI, which is dependent on the starting date or ending date of the freezing or thawing season; the angular frequency of sin function is set as $2\pi/12$ which is back-calculated by assuming period of 12 month.

Using equation(13- 1) and (13- 2) with unconstrained coefficients, the site-measured IRI_{sf} and the predicted IRI_{sf} for different sites are obtained. Example of the results using data from 50-1002 and 30-8129 are shown in Figure 13- 7 and Figure 13- 8, respectively. Here the unconstrained coefficients in (13- 2) were determined by regression using site-measured IRI_{sf} with smallest root mean square error. However, the coefficients in (13- 2) should be constrained by environmental factors. To determine the constrains of the coefficients in (13- 2), the subsequent studies were performed.

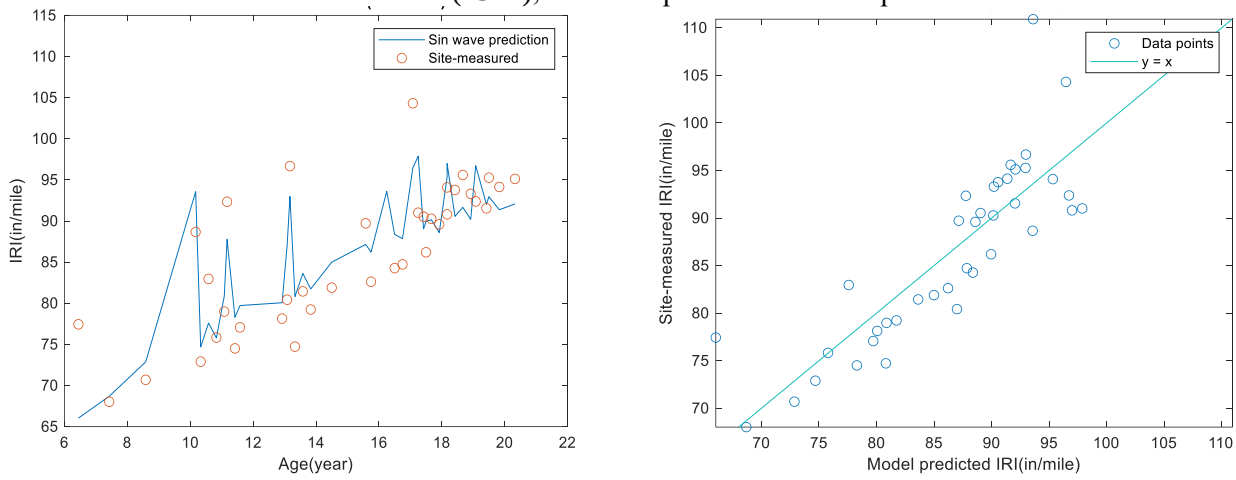

Figure 13- 7 Comparison site-measured and predicted IRI_{sf} for section 50-1002: a) time-series process; b) 1:1 chart

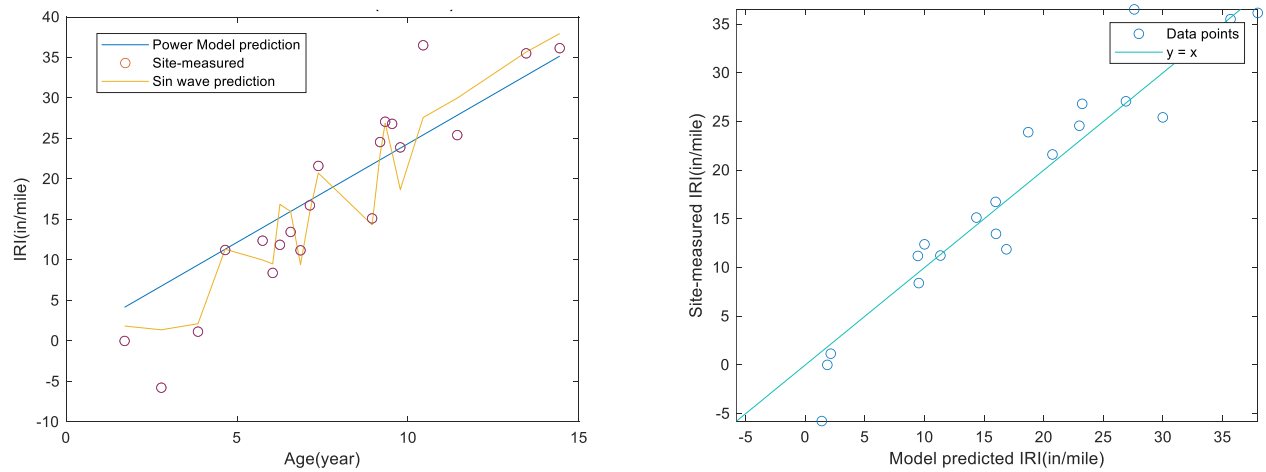

Figure 13- 8 Comparison site-measured and predicted IRI_{sf} for section 30-8129: a) time-series process; b) 1:1 chart

13.4.2.1 Coefficients beta evaluation

For the new IRI site factor equation, the coefficient beta, as the power term of the pavement age, is found related to pavement structure. To identify the influence of the different factors on beta value, the power law regression ($IRI_{sf} = a * age^{beta}$) of the site measured IRI vs. pavement age were performed using 460 sets of data from 66 sections and 20 states. Compared with Table 13- 1, more data of 66 sections were collected from the MATLAB processed LTPP database as presented in Appendix 12. The selected section information is presented in Table 13- 2. Unlike the sections selected in Table 13- 1, the Table 13- 2 contains data that did not require 3 adjacent data points within 1 year. Whereas the new data assembled in Table 13- 2 requires: 1) section has minimum 0.4m frost depth and 20% fine

content; 2) all data need to be within the duration of construction #1 to avoid the impacts of the maintenance; 3) has at least 4 sets of site-measured IRI vs. age.

Table 13- 2 The 66 sections selected to study the effects of pavement design on the coefficient beta

State code	SHRP_ID	State name	Pavement thickness (ft)	Subgrade fine content (%)	Annual precipitation(in)
8	1029	Colorado	1.74	38.40	13.25
8	7036	Colorado	1.28	56.00	24.46
8	7783	Colorado	2.56	72.50	15.51
23	1012	Maine	3.51	22.10	50.51
26	0115	Michigan	1.31	57.50	35.38
26	0118	Michigan	1.64	67.70	35.38
26	0123	Michigan	1.44	67.70	35.38
26	1010	Michigan	2.72	61.20	35.38
26	1012	Michigan	2.72	52.70	51.14
27	1087	Minnesota	1.31	52.70	39.47
30	0116	Montana	1.44	26.35	37.71
30	0119	Montana	1.38	26.35	31.98
30	0124	Montana	2.07	27.80	15.20
30	1001	Montana	2.17	24.80	15.20
30	7066	Montana	2.03	66.60	22.29
30	8129	Montana	2.17	27.70	24.02
36	0801	New York	1.12	57.75	20.78
36	0802	New York	1.48	28.93	40.33
36	0859	New York	1.57	22.03	30.30
36	1011	New York	2.07	20.87	30.30
39	0106	Ohio	1.54	20.87	48.04
39	0108	Ohio	1.54	70.60	42.95
39	0110	Ohio	1.25	70.60	50.72
39	0111	Ohio	1.28	75.20	40.17
39	0159	Ohio	2.46	70.50	38.18
39	0160	Ohio	1.57	70.50	47.64
39	0902	Ohio	2.20	67.50	47.64
39	7021	Ohio	1.48	75.57	47.64
42	1599	Pennsylvania	1.74	75.57	42.49
42	1605	Pennsylvania	2.03	48.40	57.43
42	7025	Pennsylvania	1.80	30.60	58.08
46	0803	South Dakota	1.02	42.85	59.57
46	0804	South Dakota	1.61	34.65	21.15
49	1001	Utah	0.95	54.18	19.02
49	1004	Utah	1.41	20.45	14.79
49	1005	Utah	1.97	24.20	16.21
49	1006	Utah	1.64	24.20	20.21
49	1007	Utah	1.21	27.60	13.30
49	A332	Utah	1.08	27.60	14.39
49	C331	Utah	3.15	17.00	16.21
53	1501	Washington	1.38	20.00	13.30
53	6020	Washington	1.97	42.05	16.22
53	6049	Washington	2.40	34.85	34.33
53	6056	Washington	1.48	34.85	43.07
53	7322	Washington	1.64	31.20	28.53
55	0122	Wisconsin	2.36	52.95	25.57
81	1803	Alberta	1.28	23.00	40.07
81	1805	Alberta	1.67	23.00	55.19
56	2015	Wyoming	2.30	42.20	16.90
56	2017	Wyoming	1.15	36.90	16.20
56	2037	Wyoming	1.67	28.65	18.02
56	6031	Wyoming	1.15	28.65	22.56

82	1005	British Columbia	2.13	39.60	15.18
83	1801	Manitoba	1.94	24.60	19.91
87	0961	Ontario	1.21	25.35	22.64
87	1620	Ontario	2.85	32.40	45.86
87	1622	Ontario	3.22	32.40	44.33
87	1680	Ontario	3.18	48.20	49.09
87	1806	Ontario	4.23	48.20	36.71
87	2811	Ontario	1.38	66.50	34.12
87	2812	Ontario	1.21	79.15	39.72
88	1645	Prince Edward Island	1.80	78.70	36.03
89	2011	Quebec	3.77	33.45	53.79
90	6400	Saskatchewan	0.85	40.30	64.44
90	6405	Saskatchewan	1.18	21.40	16.70
90	6801	Saskatchewan	0.92	22.60	16.53

The plot of the regressed beta values vs. pavement thickness is shown in Figure 13- 9. Based on the results, the following fitting equation is proposed:

$$beta = \frac{0.17}{thickness(m)} = \frac{0.558}{thickness(ft)} \quad \textbf{(13- 4)}$$

where thickness is the total thickness of the pavement structure from the subgrade top to pavement surface. Apparently, the power term tends to decrease with increased thickness of the pavement. This is intuitively reasonable, because thicker pavement structure tends to mitigate frost heave impacts with more stronger pavement structure. As a result, in thicker road sections, IRI increment with time will be smaller than sections with thinner pavement structures.

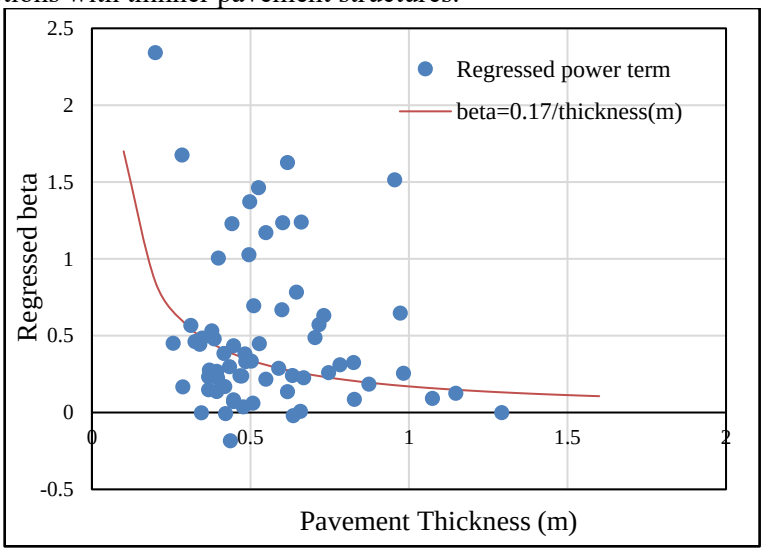

Figure 13- 9 Pavement thickness vs. regressed beta of the 66 sections

13.4.2.2 Coefficients eta, gamma, DF_T, and $IRI_{sf_{max}}$ evaluation

In order to calibrate Equation (13- 1) to (13- 3) to obtain the constrained coefficients, a series of calibrations were performed. 388 sets of data were selected from 50 road sections that can be influenced by frost heave. Data of different construction numbers were also included. All sections have at least 3 sets of age vs. FC, TC, RD, and IRI data and requires at least 20% fine content. The information of road sections is presented in Table 13- 3 below.

Table 13- 3 Summary of road section information for data used for overall calibration

State_code|SHRP_ID| Construction#	State name	Fine content (%)	Frost depth by Yoder and Witczak, 1975 (ft)	Average annual precipitation (in)	Pavement Thickness (ft)
8|1029|5	Colorado	38.40	3.21	16.59	1.98
26|0115|1	Michigan	56.70	3.43	35.02	1.30
26|0123|1	Michigan	60.20	3.43	35.02	1.43
30|0116|1	Montana	30.45	3.18	19.95	1.45
30|0119|1	Montana	29.30	3.18	19.95	1.38
30|0124|1	Montana	40.70	3.18	19.95	2.08
30|7075|3	Montana	27.70	3.12	24.33	3.30
30|7088|2	Montana	26.55	4.27	25.94	2.28
30|8129|1	Montana	57.75	3.74	18.80	2.17
30|8129|2	Montana	57.75	3.73	19.73	2.52
36|0801|1	New York	28.92	2.20	39.00	1.12
36|0802|1	New York	21.90	2.17	39.40	1.47
36|0859|1	New York	17.37	2.18	38.61	1.58
39|0106|1	Ohio	72.10	2.86	52.34	1.53
39|0111|1	Ohio	69.70	2.82	53.33	1.29
39|0160|1	Ohio	66.40	2.87	50.96	1.57
42|0608|2	Pennsylvania	31.93	3.47	53.30	2.29
42|1597|2	Pennsylvania	46.50	4.14	44.09	1.94
42|1597|6	Pennsylvania	46.50	4.07	49.51	2.37
42|1605|2	Pennsylvania	30.60	2.87	44.69	2.25
42|7037|3	Pennsylvania	36.85	3.00	46.84	2.08
46|0803|1	South Dakota	29.02	4.51	23.61	1.03
46|0804|1	South Dakota	29.02	4.32	20.96	1.59
49|0803|2	Utah	31.80	4.66	38.09	4.50
49|0804|2	Utah	40.40	4.66	38.09	5.03
49|1001|1	Utah	20.45	1.68	11.47	0.94
49|1001|2	Utah	20.45	1.86	12.48	0.98
49|1004|1	Utah	24.20	3.02	19.87	1.43
49|1006|1	Utah	27.75	2.56	14.45	1.63
49|1008|2	Utah	61.10	2.88	14.39	1.23
53|1002|1	Washington	64.30	1.35	24.00	1.05
53|1501|1	Washington	42.05	2.40	18.76	1.37
53|6056|2	Washington	53.80	2.14	24.61	1.68
55|0122|1	Wisconsin	23.00	4.78	40.76	2.35
55|A903|3	Wisconsin	29.00	3.48	36.52	1.93
55|A909|3	Wisconsin	26.00	3.67	39.07	2.09
56|1007|2	Wyoming	23.80	3.60	23.96	0.75
56|2015|1	Wyoming	36.90	3.23	22.40	2.31
56|2017|1	Wyoming	28.65	3.12	21.40	1.14
56|7772|6	Wyoming	20.60	3.20	12.85	1.68
56|7775|1	Wyoming	22.10	4.18	14.76	0.96
83|0502|3	Manitoba	25.83	5.69	24.98	1.36
83|0502|4	Manitoba	25.83	6.40	28.73	1.36
83|0502|6	Manitoba	25.83	6.06	30.54	1.40
83|0506|3	Manitoba	45.20	6.11	27.23	1.74
83|0506|5	Manitoba	45.20	6.06	30.54	1.78
83|0509|3	Manitoba	42.70	6.16	28.69	1.63
83|1801|1	Manitoba	19.70	6.57	20.04	1.93
83|1801|5	Manitoba	19.70	6.11	18.84	1.93
83|6454|14	Manitoba	42.50	6.36	30.34	1.08
87|0961|1	Ontario	33.00	5.41	45.33	1.21
87|1620|3	Ontario	79.60	3.69	39.72	3.23
87|1622|1	Ontario	48.20	4.80	48.18	3.23

87|1622|2	Ontario	48.20	4.11	45.66	3.38
87|1806|3	Ontario	75.50	3.39	37.03	4.20
87|2811|1	Ontario	79.10	3.25	34.52	1.38
90|6405|1	Saskatchewan	24.45	6.48	22.51	1.19
90|6405|2	Saskatchewan	24.45	6.43	20.73	1.19

Using the collected data from sections as shown in Table 13- 3, a series of regressions of Equation (13- 1) to (13- 3) were performed. Through trials, the parameters c_1, c_2, and c_3 for FC, TC and RD are initially assumed as 0.1, 0.0009, and 10 separately. Note that this assumption is made merely for calibration of the other coefficients. Values of c_1, c_2, and c_3 will be further calibrated in the final step. Next, site-monitored IRI_{sf} is back-calculated by input of IRI_0 and distress data with assumed c_1, c_2, and c_3. Using the back-calculated IRI_{sf}, single-section-based regressions were performed for all the sections presented Table 13- 3.

The result example of 9 sections were shown in Figure 13- 10 below. The results in Figure 13- 10 verified the Equation (13- 2) and (13- 1) were able to predict site-monitored IRI_{sf} and IRI respectively.

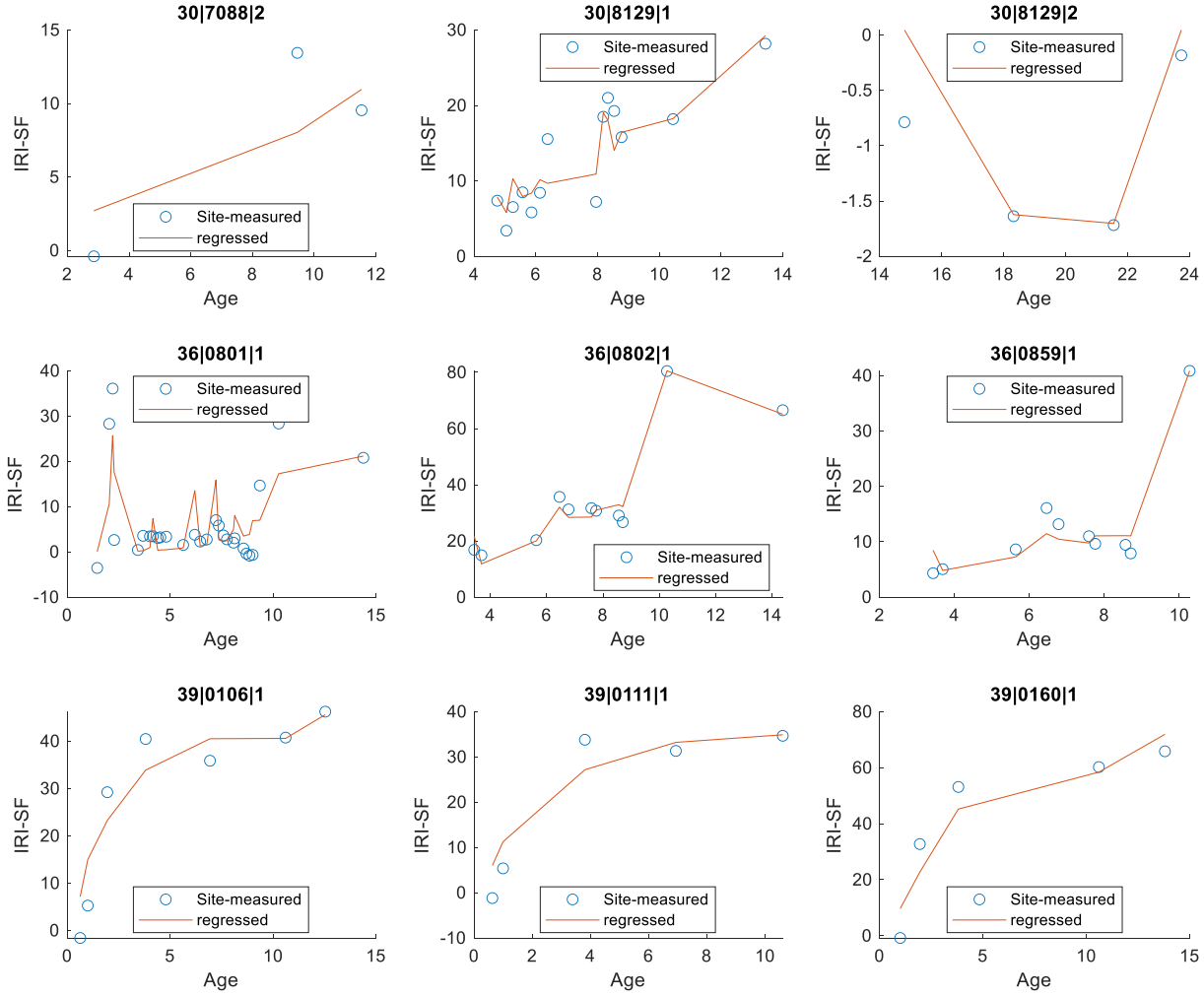

(a)

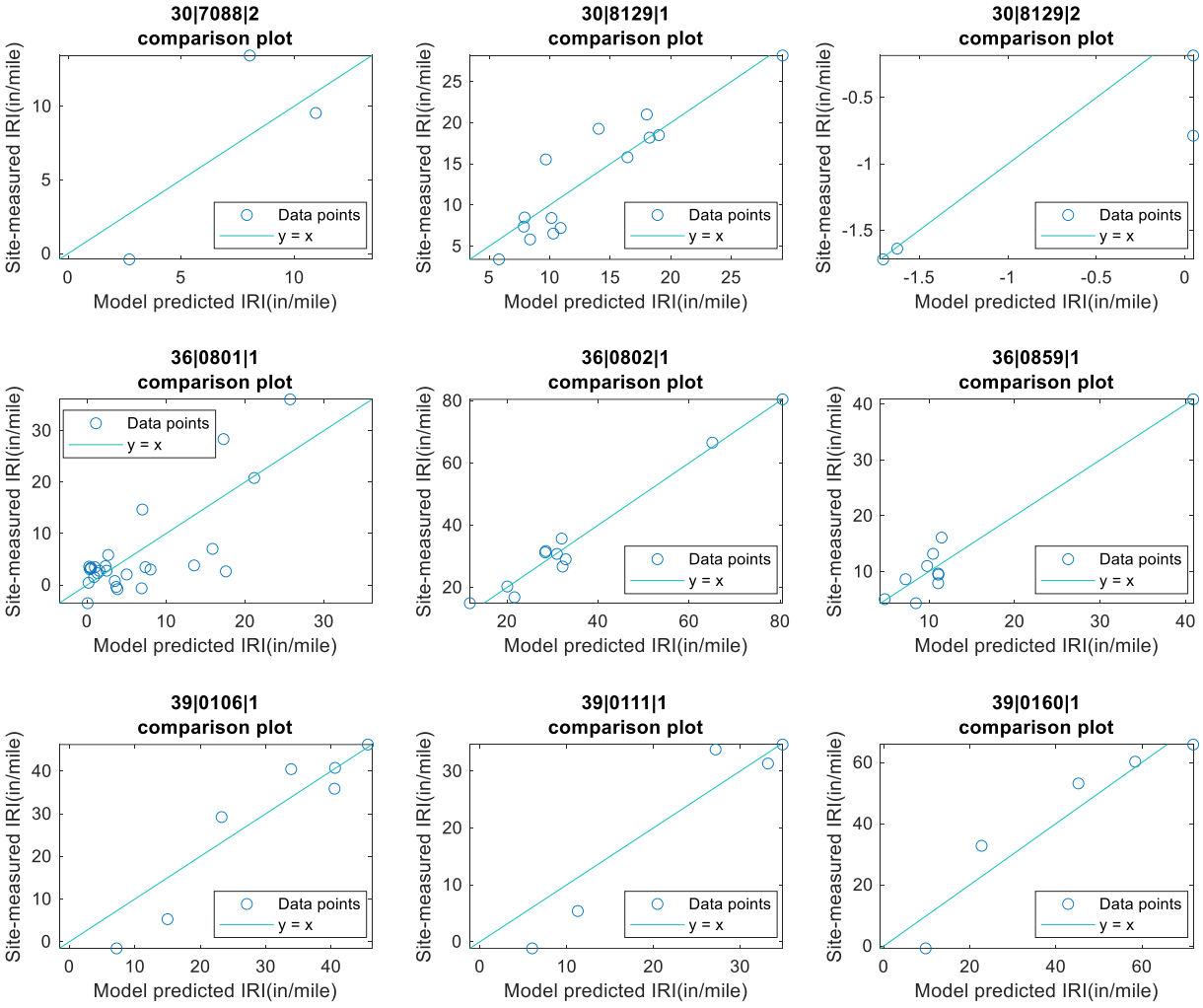

(b)

Figure 13- 10 Examples of regression result on 9 selected sections in Table 7: (a) plots of age vs. IRI_{sf}; (b) comparison plots between model predicted and site-measured IRI

To obtain simple and generally applicable coefficients, detailed analysis of coefficient of eta, gamma and $IRI_{sf_{max}}$ were conducted. Replacing beta with 0.558/thickness (ft) in Equation (13- 2), sensitivity analysis of parameter eta and gamma were performed. It was found that eta primarily affects the position of the peaks while gamma influences the magnitude of the fluctuations of the IRI_{sf} vs. time curve.

According to the observation of site measured IRI with time, some abrupt IRI jump usually occurred between the start of February and the end of May. This implies the freezing and thawing processes may cause significant seasonal increases in IRI_{sf}. Assuming the IRI jump occurred in the end of March, using period of 1 year, the phase term eta of the sine function was back-calculated as 0.35. The regressed results showed that the parameter $IRI_{sf_{ref}}$, gamma, and beta can all be influenced by each other.

Therefore, when beta is set as 0.558/thickness(ft), to avoid the influence between gamma and $IRI_{sf_{ref}}$ of the regression, gamma is set as a constant value of 0.0005, which means the true magnitude of the IRI fluctuation is controlled by $IRI_{sf_{ref}}$. According to the physical meaning of DF_T, its value should be close to 1 and 0 when thickness is smaller and larger than some threshold value separately. Hence, the following equation is proposed to evaluate DF_T:

$$DF_T = -0.188 * ln(0.3048 * thickness(ft)) + 0.131 \quad \textbf{(13- 5)}$$

where thickness is the total pavement structure thickness in ft.

The parameter $IRI_{sf_{max}}$, is the site factor induced IRI in ground soil with no pavement structure. It is associated with the magnitudes of differential frost heaves. It is related to soil properties (SP, density, water content) and climatic conditions as well as their variabilities. According to regression analyses, the $IRI_{sf_{max}}$ shows positive correlation with silt percentage of the subgrade soil, the annual precipitation and the annual freezing index in Figure 13- 11. These are reasonable because increasing percentage of silt corresponds to higher frost susceptibility of the subgrade. Larger annual precipitation provides more water supply to cause frost heave. Also, the larger the annual freezing index, the deeper the frost depth. Higher annual precipitation, larger freezing index and higher silt content are all associated with more frost heave.

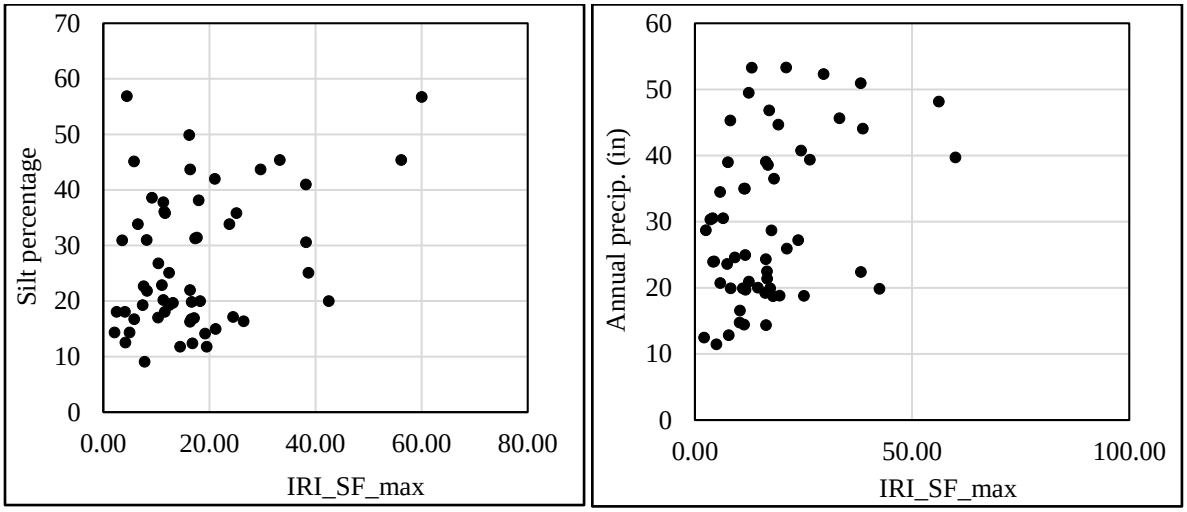

(a) (b)

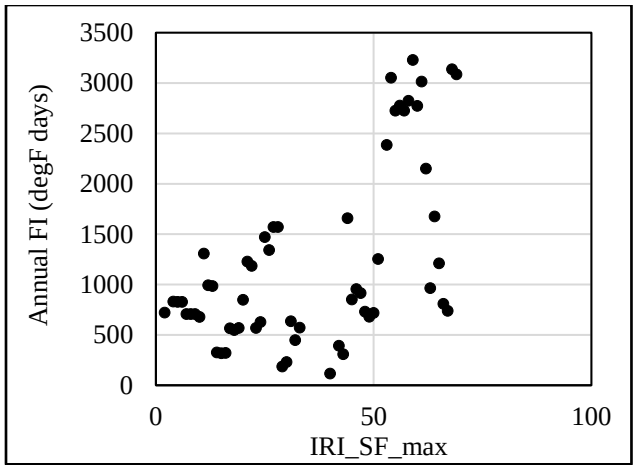

(c)

Figure 13- 11 The positive correlation of $IRI_{sf_{max}}$ versus a) Silt content (%); b) Annual precipitation (in); c) Annual freezing index (degF days)

Based on the above conclusions, the following equation is proposed to compute the $IRI_{sf_{max}}$:

$$IRI_{sf_{max}} = e_1 * ln(e_2 * FI + 1) * ln(e_3 * Precip + 1) * ln(e_4 * Silt_{percentage} + 1) \quad \textbf{(13- 6)}$$

where e_1 to e_4 are the calibration coefficients.

13.4.3 Summary of the empirical IRI equation for flexible pavement

After calibration, the determined empirical IRI equations for flexible pavement are presented below:

$$IRI = IRI_0 + IRI_{SF} + 0.292(FC_{Total}) + 0.0038(TC) + 11.28(RD) \quad \textbf{(13- 7)}$$

$$\mathrm{IRI_{sf}} = \mathrm{IRI_{sf_{max}}} * DF_T * [\mathrm{age}^{\frac{0.558}{\mathrm{thickness}}} + 0.0005 * \mathrm{FI_{accum}} * \sin(\pi * \frac{\mathrm{month}}{6} + 0.35)] \quad \textbf{(13- 8)}$$

$$DF_T = -0.188 * LN(0.3048 * thickness) + 0.131 \quad \textbf{(13- 9)}$$

$$IRI_{sf_{max}} = 0.8 * ln(0.2 * FI + 1) * ln(0.535 * Precip + 1) * ln(0.06 * Silt_{percentage} + 1) \quad \textbf{(13- 10)}$$

Using Equation (13- 7) to (13- 10), the IRI were predicted and compared with the site-measured IRI. To show the improvements of the new empirical model, the 1-1 plot comparison between the new model and MEPDG model are shown in Figure 13- 12 . The MEPDG model predicted IRI_{sf} is evaluated based on Method 9. Details of method 9 are presented in Appendix 12. As shown in Figure 13- 12, the new empirical model showed much better performance with $R^2 = 0.6312$.

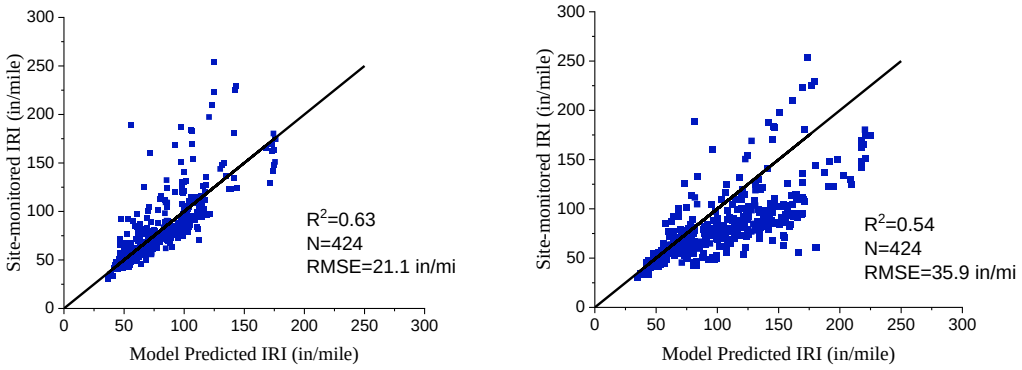

Figure 13- 12 Site-measured IRI_{sf} vs. model predicted IRI_{sf} evaluated via: (a) model equations (13- 7) to (13- 10); (b) the MEPDG model for flexible pavement with Method 9

13.5 The MEPDG IRI model for rigid pavement

In LTPP database, the rigid pavement surface can be classified into three categories: 1) HMA Overlays of Rigid Pavements; 2) Jointed Plain Concrete Pavements (JPCP); 3) Continuous Reinforced Concrete Pavements (CRCP)

The IRI prediction equation for HMA Overlays of Rigid Pavements is*:*

$$IRI = IRI_0 + 0.00825(SF) + 0.575(FC_{Total}) + 0.0014(TC) + 40.8(RD) \quad \textbf{(13- 11)}$$

The definition of each term is same as the corresponding terms of Equation (13- 1). It seems that the SF equation is not provided for HMA Overlays of Rigid Pavements in MEPDG 2008, 2015 and 2020 manual. It is likely that the same SF equation is used for both flexible pavement and HMA Overlays of Rigid Pavement in the MEPDG manuals.

The IRI prediction equation for Jointed Plain Concrete Pavements (JPCP) is:

$$IRI = IRI_0 + 0.8203 \cdot CRK + 0.4417 \cdot SPALL + 1.4929 \cdot TFAULT + 25.24 \cdot SF \quad \textbf{(13- 12)}$$

where *CRK* is the Percent slabs with transverse cracks (all severities), *SPALL* is the Percentage of joints with spalling (medium and high severities), *TFAULT* is the total joint faulting accumulated per mile (in), and *SF* is the Site factor, which is calculated in accordance with the following equation:

$$SF = AGE\ (1 + 0.5556 \cdot FI)(1 + P_{200}) \cdot 10^{-6} \quad \textbf{(13- 13)}$$

where *age* is the pavement age (yr), *FI* is the Average annual freezing index (degF days), and P_{200} is the Percent passing the 0.075 mm sieve. For SPALL and TFAULT variables, no data is found in the LTPP neither in the MON_DIS_JPCC_REV nor MON_DIS_JPCC_CRACK_INDEX spreadsheets. As a result, it is not feasible to conduct a calibration analysis to the MEPDG IRI equation for JPCP. So, the team does not do any calibration for sections with JPCP surface.

The IRI prediction equation for Continuous Reinforced Concrete Pavements (CRCP) is:

$$IRI = IRI_0 + 3.15 \cdot PO + 28.35 \cdot SF \quad \textbf{(13- 14)}$$

where *PO* is the Number of medium- and high-severity punchouts/mi, and *SF* is the Site factor, which is calculated in accordance with the following equation:

$$SF = AGE\ (1 + 0.556 \cdot FI)(1 + P_{200}) \cdot 10^{-6} \quad \textbf{(13- 15)}$$

Like the new IRI models for flexible pavement discussed before, the empirical IRI prediction models are proposed for HMA overlay and CRCP pavement. The way to consider IRI_0 and age are well discussed in Appendix 12, which is also used for the following empirical model calculations.

13.6 The new IRI model for HMA overlay pavement

13.6.1 Data collection summary for HMA overlay pavement

The LTPP data used for HMA overlay equation calibration is collected and summarized as shown in Table 13- 4. The sections are selected following these criteria:

1) Having available IRI, IRI_0, FC, TC, and RD at same recording date (data difference is within 180 days)
2) Subgrade with fine content larger than 10% and wPI less than 10
3) At least 3 available values of IRI
4) Sections are believed to be frost susceptible

Based on the above criteria, very limited data from 17 sections were collected.

Table 13- 4 The 17 HMA overlay sections selected for analysis

STATE_CODE	STATE_CODE_EXP	SHRP_ID	Surface type	Data set number
9	Connecticut	5001	CRCP with AC overlay	3
17	Illinois	0603	JPCC with AC overlay	3
17	Illinois	0603	JPCC with AC overlay	3
17	Illinois	0607	JPCC with AC overlay	4
17	Illinois	5151	CRCP with AC overlay	3
19	Iowa	0605	JPCC with AC overlay	4
19	Iowa	3006	JPCC with AC overlay	4
19	Iowa	3055	JPCC with AC overlay	4
29	Missouri	0603	JPCC with AC overlay	4
42	Pennsylvania	0603	JPCC with AC overlay	7
42	Pennsylvania	0608	JPCC with AC overlay	7
42	Pennsylvania	1691	JPCC with AC overlay	5
50	Vermont	1682	JPCC with AC overlay	4
54	West Virginia	4004	JPCC with AC overlay	3
55	Wisconsin	A907	JPCC with AC overlay	3
55	Wisconsin	A908	JPCC with AC overlay	3
55	Wisconsin	A909	JPCC with AC overlay	4

13.6.2 The model development and calibration

In Equation (13- 12), the IRI is contribute to IRI_0, IRI_{sf}, and other distress terms. Since IRI_0 denotes the initial IRI value, the difference between the IRI and IRI_0 can be defined as the general increment of IRI after the date of IRI_0, hereafter refer to as IRI_increment. In the collected data shown in Table 13- 4, only 9 sections have more than 3 data points. Here the age vs. IRI increment of these 9 sections are shown in Figure 13- 13. It is found the general IRI variation with time has two stages: 1) the IRI keeps constant or slightly fluctuated around 0 for several years after the construction of overlay or maintenance; 2) IRI start to increase apparently with time. The stage of relative flat IRI increments may indicate relatively strong concrete strength conditions below the overlay. As time goes on, the repeated frost heave and thaw settlement can gradually decrease the stiffness of concrete slab and make it broken. When concrete strength becomes low, the overlay will be impacted easily by frost behavior of the subgrade soil. As a result, the IRI increment started to increase apparently. Here the age when IRI increment start to increase (end of stage 1 or start of stage 2) is defined as age_{inc}. The age of overlay is defined as the time difference between the age_{inc} and the age when overlay is constructed, which is written as $t_{overlay}$. According to the features of the two stage IRI increment and referring the flexible pavement IRI model equation (13- 1), the following equations are proposed and calibrated as the new IRI prediction model for HMA overlay pavement:

$$IRI = IRI_0 + IRI_{SF} + c_1(FC_{Total}) + c_2(TC) + c_3(RD) \quad \textbf{(13- 16)}$$

where c_1, c_2, and c_3 are calibration coefficients of pavement distress terms. Their values are assumed to be same as the new empirical flexible pavement model as presented before. IRI_{SF} is the IRI increment caused by site factors (or frost and thawing influence). The new calibration equations for the site factor due to frost heave is proposed as:

$$\mathrm{IRI_{sf}} = \begin{cases} 0 & when\ (age < age_{inc}) \\ \mathrm{IRI_{sf_{ref}}} * (age - age_{inc})^{beta} & when\ (age > age_{inc}) \end{cases} \quad \textbf{(13- 17)}$$

$$\mathrm{IRI}_{sf_{ref}} = \mathrm{IRI_{sf_{max}}} * DF_T \quad \textbf{(13- 18)}$$

The definition and physical meaning of parameter beta, IRI_sf_max, and DF_T are same as the empirical flexible pavement model, but their values are evaluated by different equations.

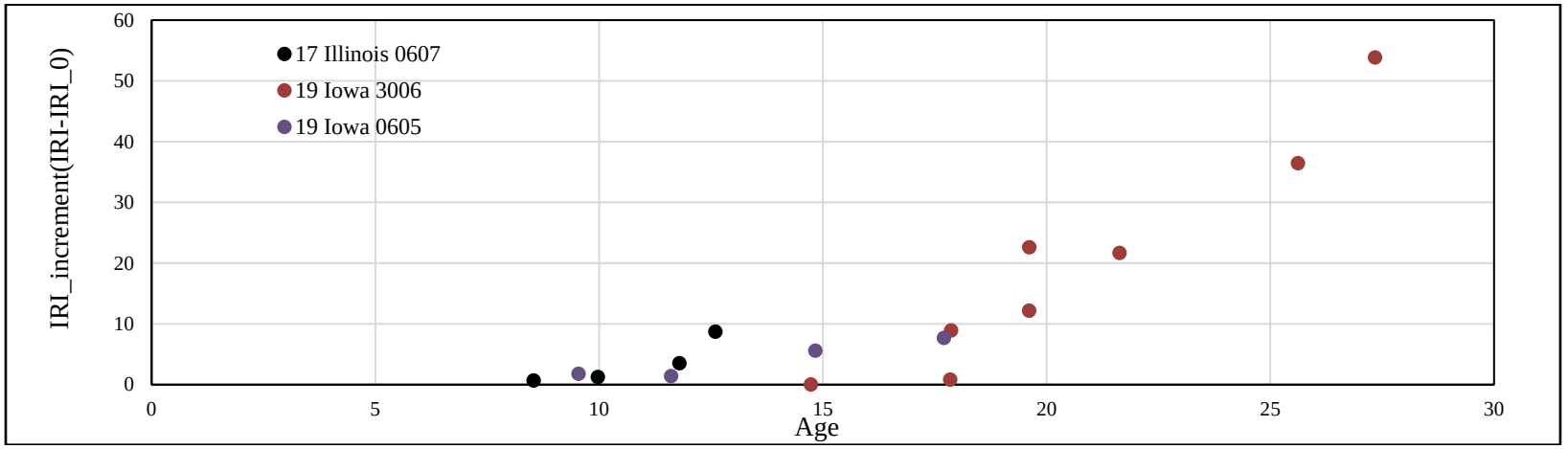
IRI_increment(IRI-IRI_0)
60
50
40
30
20
10
0
0
5
10
15
20
25
30
Age
17 Illinois 0607
19 Iowa 3006
19 Iowa 0605

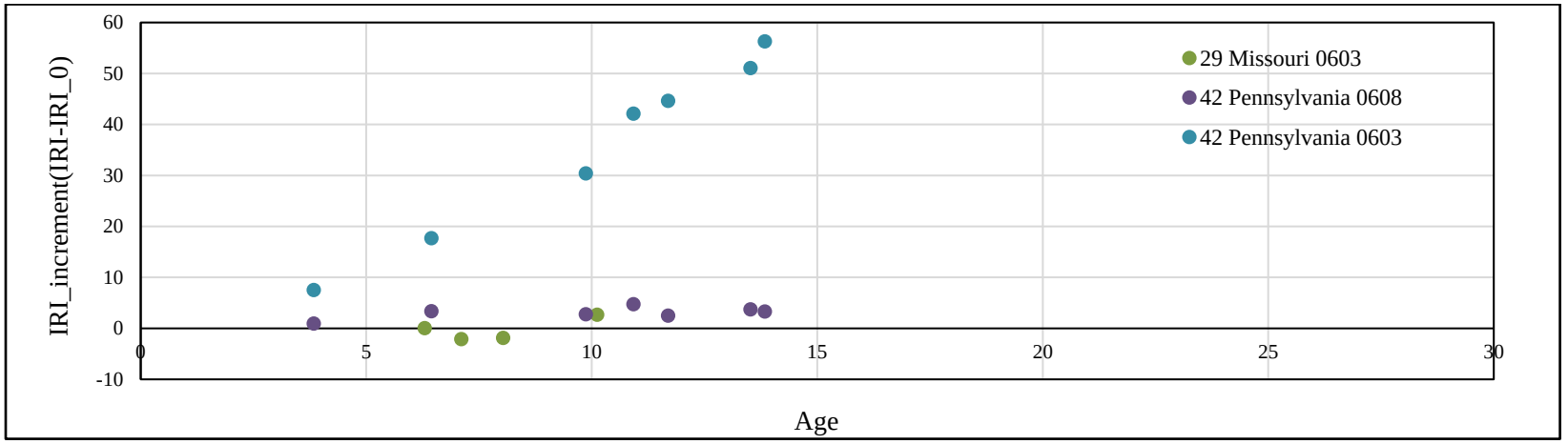
IRI_increment(IRI-IRI_0)
60
50
40
30
20
10
0
-10
0
5
10
15
20
25
30
Age
29 Missouri 0603
42 Pennsylvania 0608
42 Pennsylvania 0603

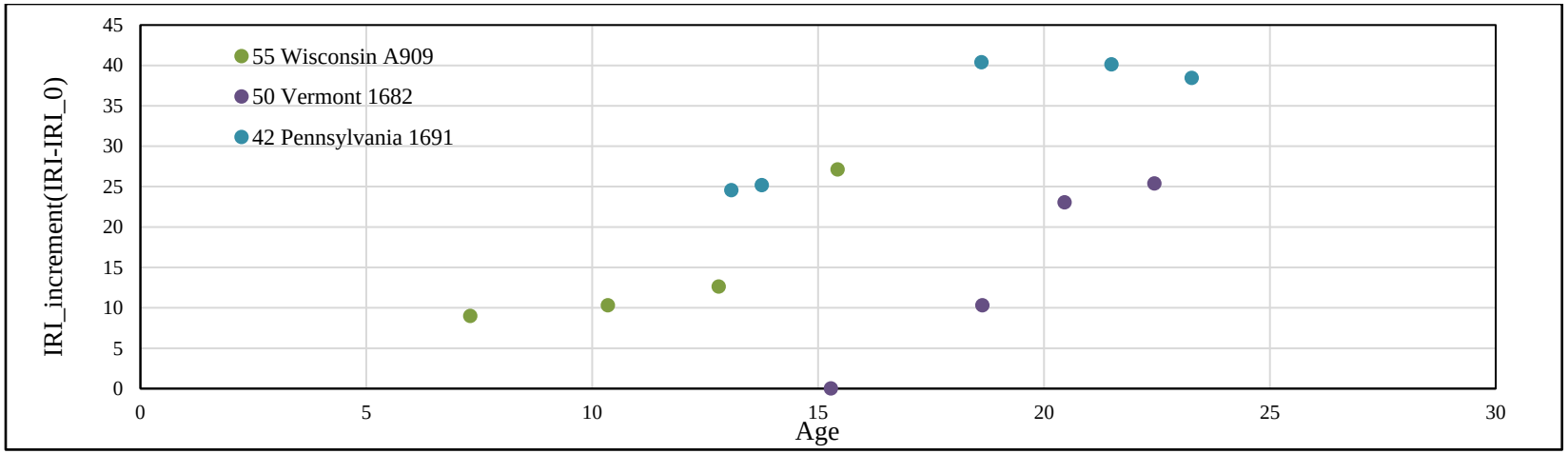

Figure 13- 13 Age vs. IRI_increment for the 9 sections with HMA overlays of rigid pavements

Through several regression trials, it is found that the age_{inc} is related to total pavement thickness before overlay ($L_0, in\ ft$) and the age of overlay ($t_{overlay}$, in year). The following equation is proposed to evaluate age_{inc}:

$$age_{inc} = (0.01728 * ln(L_0/3.28084) + 0.7374) * t_{overlay}^{1.079} + 6.099 \quad \textbf{(13- 19)}$$

Since the construction of HMA overlay pavement usually includes two separate stages: construction of rigid pavement and construction of asphalt overlay, which is different from flexible pavement, its IRI prediction model should also be different from the flexible pavement and take the two stages influence into account. This is the reason why $t_{overlay}$ and L_0 get involved. Like the flexible pavement IRI model, similar regression analysis for HMA overlay pavement were conducted to determine the expressions of beta, $\mathrm{IRI}_{\mathrm{sf}_{\max}}$, and DF_T. Then the following equations are proposed:

$$beta = 0.206 * thickness_{AC}^{-1.62} \quad \textbf{(13- 20)}$$

$$DF_T = 0.1517 * \exp(-0.82 * L_0) \quad \textbf{(13- 21)}$$

$$\mathrm{IRI\_sf\_max} = \ln(50\mathrm{FI} + 1) * \ln(50\mathrm{Precip} + 1) * \ln\left(0.1942\mathrm{Silt}_{\mathrm{percentage}} + 1\right) \quad \textbf{(13- 22)}$$

where $thickness_{AC}$ is the thickness of the asphalt concrete in ft.

13.6.3 Summary of the new IRI model for HMA overlay pavement

The calibrated IRI equation for HMA overlay pavement are presented in equations below:

$$IRI = IRI_0 + IRI_{SF} + 0.1(FC_{Total}) + 0.0009(TC) + 10(RD) \quad \textbf{(13- 23)}$$

$$\mathrm{IRI}_{\mathrm{sf}} = \begin{cases} 0 & when\ (age < age_{inc}) \\ \mathrm{IRI}_{\mathrm{sf}_{\mathrm{ref}}} * (age - age_{inc})^{0.206 * thickness_{AC}^{-1.62}} & when\ (age > age_{inc}) \end{cases} \quad \textbf{(13- 24)}$$

$$age_{inc} = (0.01728 * ln(L_0) + 0.7374) * t_{overlay}\text{^}1.079 + 6.099 \quad \textbf{(13- 25)}$$

$$\mathrm{IRI}_{\mathrm{sf}_{\mathrm{ref}}} = 0.1517 \exp(-0.82 * \mathrm{L}_0) * \left[\ln(50\mathrm{FI} + 1) * \ln(50\mathrm{Precip} + 1) * \ln\left(0.1942\mathrm{Silt}_{\mathrm{percentage}} + 1\right)\right] \quad \textbf{(13- 26)}$$

Using equation (13- 23) to (13- 26) as well as the collected LTPP data, the IRI_{sf} were predicted and compared with the site-measured IRI_{sf}. The examples the predicted IRI_{sf} of 8 sections are shown in Figure 13- 14. The results in Figure 13- 14 indicates that Equation (13- 23) to (13- 26) can predict the site-measured IRI_{sf}. The 1-1 plot of the IRI_{sf} comparison is shown in Figure 13- 15 with $R^2 = 0.81$ and $RMSE = 6.97$.

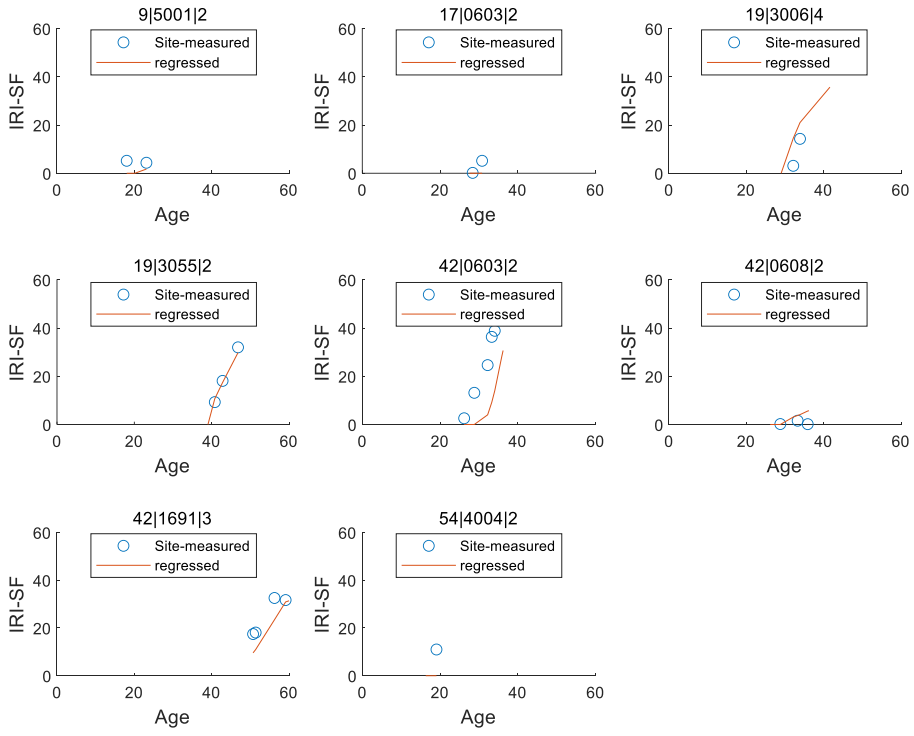

Figure 13- 14 Example plots of age vs. IRI_{sf} of model prediction and site-measurement for the 8 sections in Table 8

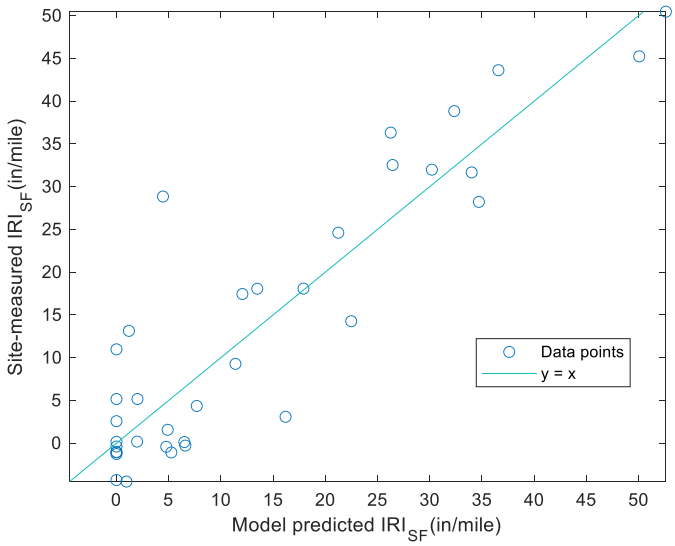

Figure 13- 15 Model predicted IRI_{sf} and site-measured IRI_{sf} comparison plot using Equation (13- 23) to (13- 26)

13.7 The new IRI model for CRCP pavement

13.7.1 Data collection summary for CRCP pavement

The LTPP data used for CRCP pavement IRI equation calibration is collected and summarized as shown in Table 13- 5. The data selection criteria for each section include:

1) Having available IRI, IRI_0, punchout at same recording date (data difference is within 180 days)
2) Subgrade with fine content larger than 10% and wPI less than 10
3) At least 3 available values of IRI
4) Sections are believed to be frost susceptible

Based on the above criteria, very limited data is collected. 239 IRI data points from 61 sets of IRI data of 16 sections are obtained, from which only 38 sets IRI data have more than 2 points. For sections that have more than 2 points with available PO data, only 15 sets of IRI data from 13 sections are available. In other words, only these sections can back calculate relative reliable IRI_{sf} for regression. (The other sections do not have PO data, cannot calculate IRI_{sf}). It is found in LTPP, most of (87 out of 96) the measured PO are 0. This can result in lots of negative sites monitored IRI_{sf}.

Table 13- 5 The 13 CRCP sections selected for analysis

STATE_CODE	SHRP_ID	STATE_CODE_EXP	Surface type	Construction#	Set number
17	5869	Illinois	CRCP	1	7
17	5869	Illinois	CRCP	2	3
19	0702	Iowa	CRCP	3	6
19	0707	Iowa	CRCP	3	5
19	5042	Iowa	CRCP	2	8
19	5046	Iowa	CRCP	4	4
27	0704	Minnesota	CRCP	2	9
27	0709	Minnesota	CRCP	2	11
41	7081	Oregon	CRCP	1	18
42	5020	Pennsylvania	CRCP	1	10
46	5020	South Dakota	CRCP	2	12
46	5040	South Dakota	CRCP	1	10
51	5009	Virginia	CRCP	1	6

13.7.2 The model development and calibration

Using data from Table 13- 5, the 9 CRCP pavement section data of age vs. site monitored IRI_{sf} are shown in Figure 13- 16. It seems the age vs. IRI_{sf} of these 9 sections are similar as HMA overlay sections with two stages: 1) the IRI keep constant or slightly fluctuated around 0 for a few years; 2) IRI start to increase with time. The physical explanations of such general IRI variation trend are similar as HMA overlay sections. For the flat IRI increments of first few years, relative high stiffness can bear the frost behavior of the soil. As time goes on, the repeated frost heave and thaw settlement may gradually decrease the strength of concrete. When concrete is broken, the impact of frost soil behavior on pavement surface will be more apparent. As a result, the IRI increment starts to increase obviously. Here the age when IRI increment start to increase (end of stage 1 or start of stage 2) is also defined as age_{inc}.

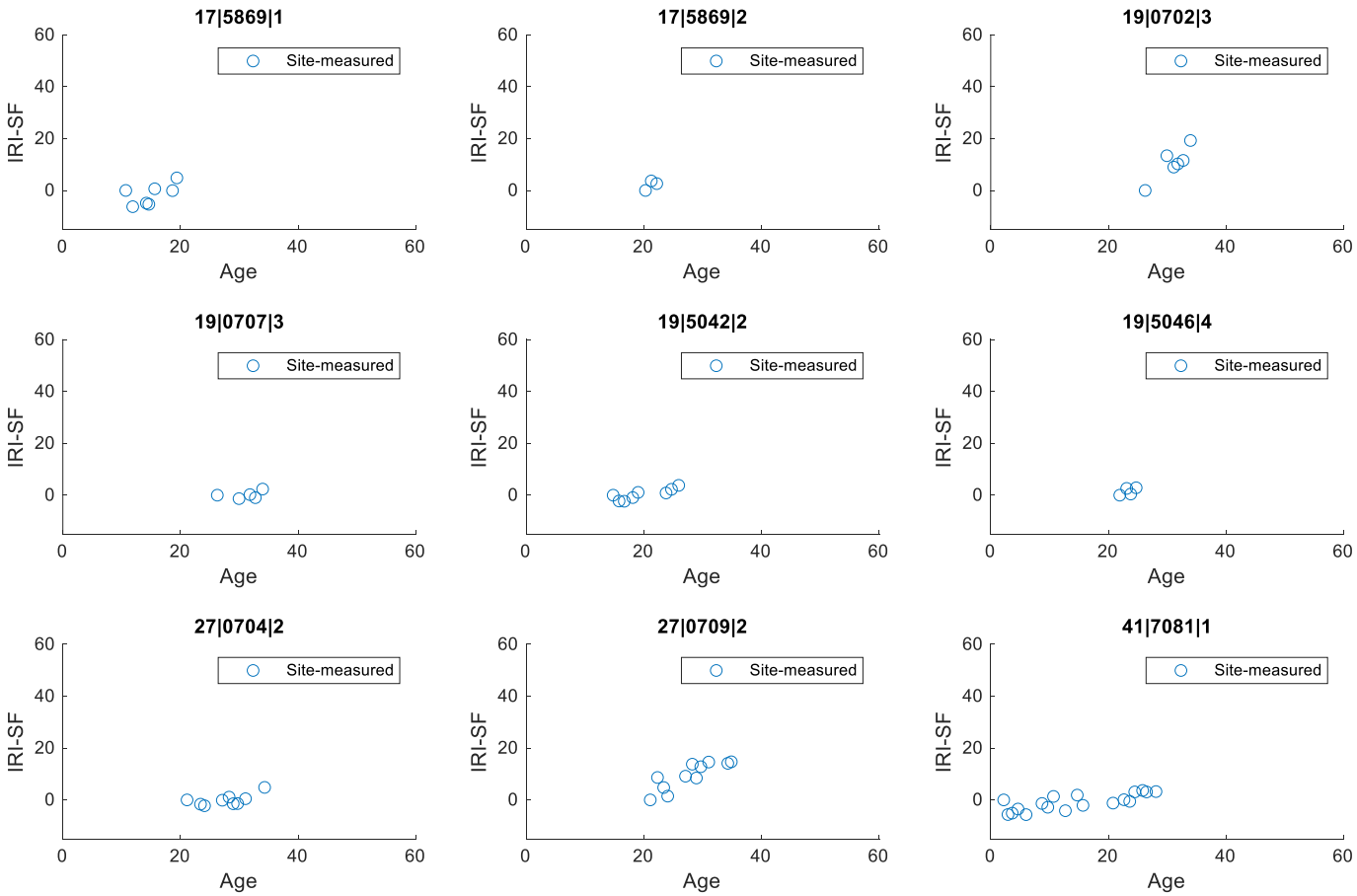

Figure 13- 16 The 9 CRCP pavement section data of age vs. IRI_{sf}

However, the IRI data features of CRCP are quite different from the data of HMA overlays. Detailed data summary of each selected CRCP section is shown in Table 13- 6. It is found among the 13 sections presented in Table 13- 6, 4 sections changed its thickness of concrete after one maintenance. The changed thickness of the section makes it hard to propose one equation (like flexible pavement) considering thickness impact on IRI_{sf} , especially when the section have more than one maintenance record (construction number larger than 2). By observing the IRI_{sf} vs. age of each section (see Figure 13- 16), only 5 sections show apparent IRI increment, which means age_{inc} is not obvious for some of the sections. Overall, the data is not good for regression-based calibration. Through the analogy of the proposed HMA overlay equation, the following equations are proposed for evaluating the IRI_{sf} for CRCP sections:

$$\mathrm{IRI_{sf}} = \begin{cases} 0 & when\ (age < age_{inc}) \\ \mathrm{IRI_{sf_{ref}}} * (age - age_{inc})^{beta} & when\ (age > age_{inc}) \end{cases} \quad \textbf{(13- 27)}$$

$$\mathrm{IRI_{sf_{ref}}} = ln(e_3 FI + 1) * ln(e_4 Precip + 1) * ln\left(e_5 Silt_{percentage} + 1\right) \quad \textbf{(13- 28)}$$

Table 13- 6 The detailed data information for the 13 CRCP sections

State|Section|Construction#	Construction time	Age of the last maintenance before IRI records	Last Maintenance	Concrete thickness right after maintenance (in)	Concrete thickness before maintenance (in)
17|5869|1	8/1/1979	-	-	8.9	8.9
17|5869|2	8/1/1979	4/15/1999	Crack Sealing	8.9	8.9
19|0702|3	9/1/1967	7/15/1992	AC Shoulder Restoration	11.9	8.0
19|0707|3	9/1/1967	7/11/1992	AC Shoulder Restoration	14.2	8.0
19|5042|2	9/1/1975	8/1/1988	Longitudinal Subdrains	8.0	8.0
19|5046|4	9/1/1975	9/1/1995	Full Depth Patching of PCC Pavement Other Than at Joint	8.3	8.3
27|0704|2	7/1/1970	9/11/1990	Longitudinal Subdrains	11.5	8.3
27|0709|2	7/1/1970	9/11/1990	Grinding Surface	12.4	8.0
41|7081|1	9/1/1988	-	-	10.4	10.4
42|5020|1	3/1/1978	-	-	9.3	9.3
46|5020|2	8/1/1972	7/22/1991	AC Shoulder Replacement	7.9	7.9
46|5040|1	7/1/1963	-	-	8.0	8.0
51|5009|1	8/1/1979	-	-	8.3	8.3

Based on the data features as discussed, to take full use of the collected data, it is assumed that the age_{inc} only occurred right after the last maintenance date. This assumption is made based on the check of the maintenance history of each section. The other maintenance before the last time maintenance is generally believed not changing the IRI apparently. Through several regression trials, the following equation of age_{inc} is proposed:

$$age_{inc} = 0.35 * \mathrm{L_b} + 2.1 * \mathrm{L_c} \quad \textbf{(13- 29)}$$

where the L_b is the thickness of the layers below the concrete slab (in inch) and L_c is the thickness of the concrete slab (in inch). The format of the proposed age_{inc} equation (13- 29) is consistent with Structure Number concept used in 1993 pavement design method. Given the regression between age_{inc} and layer

thickness data, section 42-5020 is viewed as outlier and eliminated for analysis. The 1-1 plot of age_{inc} of the left 12 sections is shown in Figure 13- 17 with $R^2 = 0.4$.

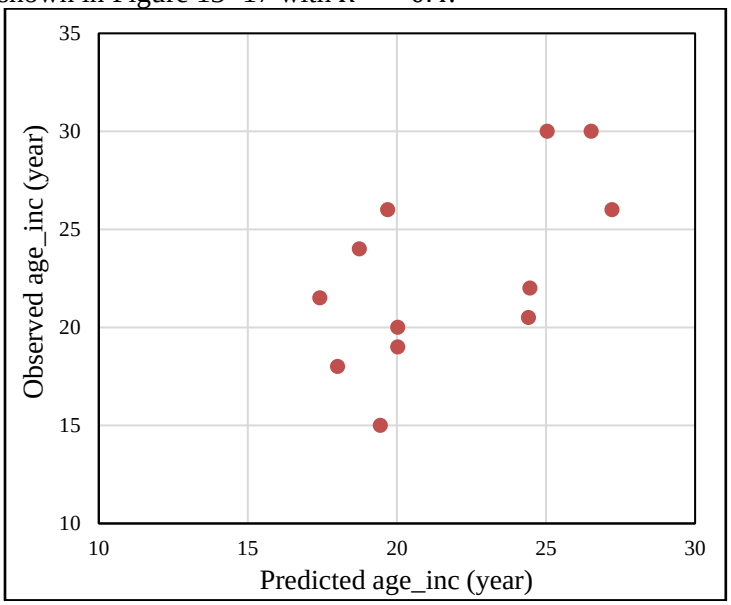

Figure 13- 17 The 1-1 plot of the predicted and observed age_{inc}

Using the determined age_{inc}, several trials were conducted to determine the best matched calibration expressions. Then the following equations are proposed:

$$\mathrm{IRI_{sf}} = \begin{cases} 0 & when\ (age < age_{inc}) \\ \mathrm{IRI_{sf_{ref}}} * (age - age_{inc})^{0.01\exp(-2*thichness)} & when\ (age > age_{inc}) \end{cases} \quad \textbf{(13- 30)}$$

$$\mathrm{IRI_{sf_{ref}}} = ln(0.01FI + 1) * ln(0.0165Precip + 1) * ln\left(9.9Silt_{percentage} + 1\right) \quad \textbf{(13- 31)}$$

To have more reasonable predictions, all negative site measured IRI_{sf} data were eliminated from the analysis during regression. Based on the above calibrated equations, the IRI_{sf} predictions were performed and compared with site data for each section as shown in Figure 13- 18. The IRI_{sf} 1-1 plot of 12 CRCP sections with R^2= 0.17 is shown in Figure 13- 19.

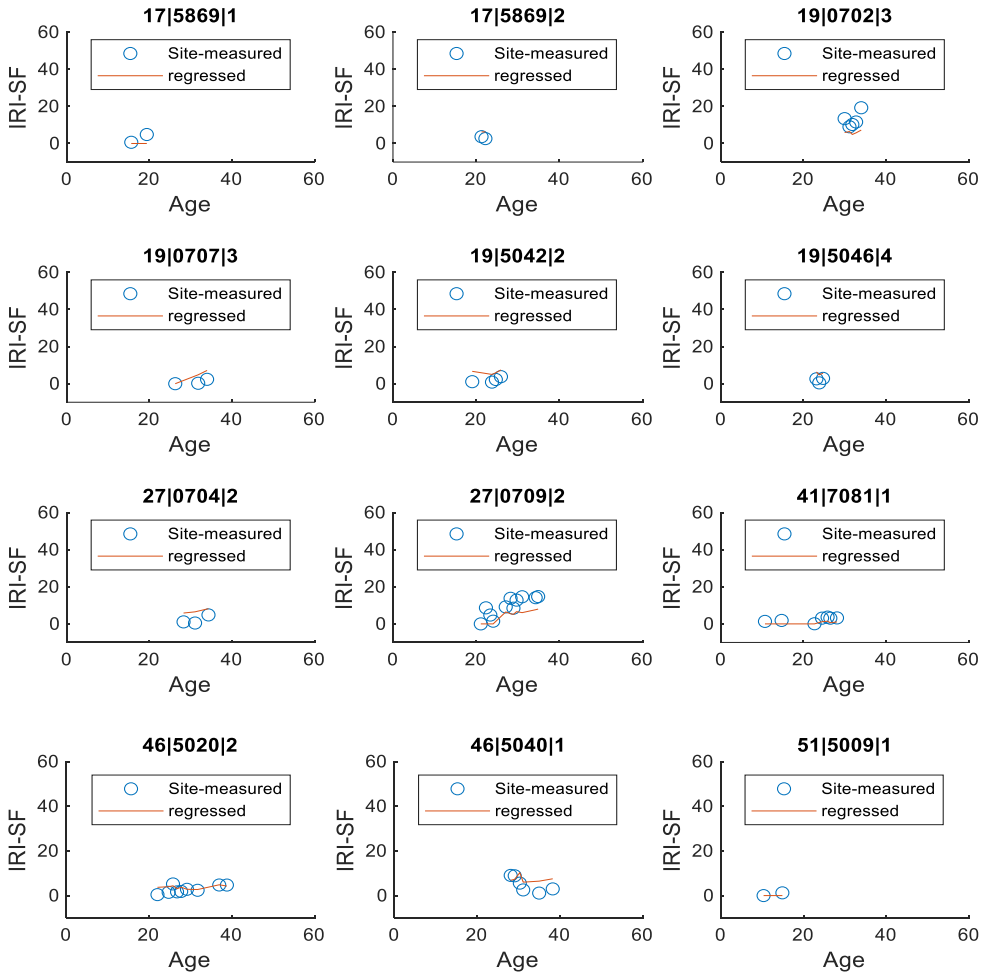

Figure 13- 18 The IRI_{sf} predictions compared with site measured IRI_{sf} for the 12 CRCP sections

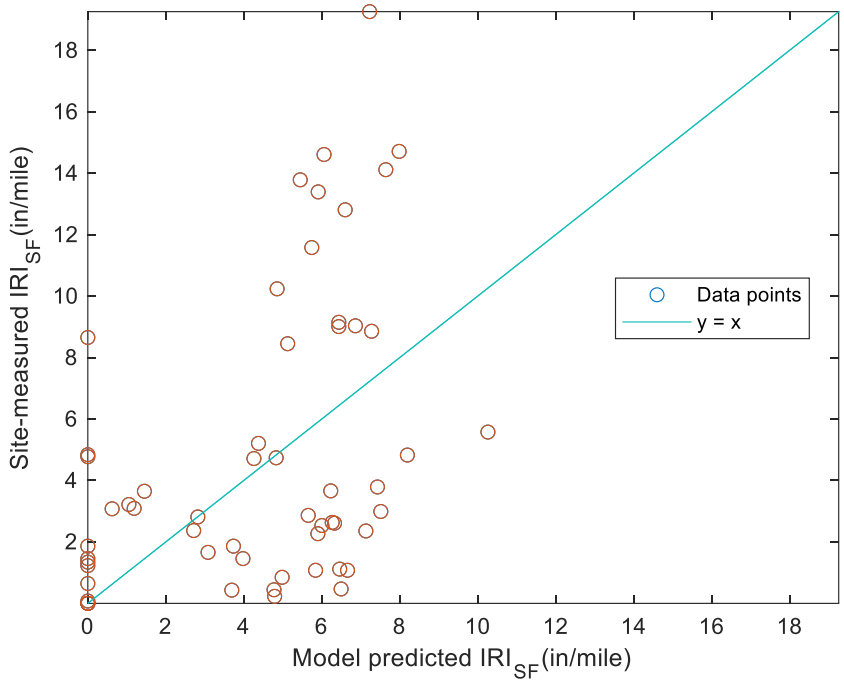

Figure 13- 19 The IRI_{sf} 1-1 plot of the 12 CRCP sections

Note that in Figure 13- 18, the predicted IRI curve may decrease a little bit with time, which is induced by the $IRI_{sf_{ref}}$ term of Equation (13- 30). Either $IRI_{sf_{ref}} or$ age can influence the IRI increment of each year. When the IRI_{sf} is less than its value of last year, it is possible that the predicted $IRI_{sf_{ref}}$ of the latter year is smaller than that of the former year. This is because of the usage of the fluctuated data with time for regression, and the regression tried to match the fluctuated data through considering the fluctuation of $IRI_{sf_{ref}}$ of different year.

Even though the CRCP pavement IRI models are proposed and calibrated, given the limited CRCP data quantity and quality, the currently calibrated model may not able to well predict the $IRI_{sf_{ref}}$. When more CRCP data are available, it may need further calibration following the same framework discussed above to get a more reliable model.

13.8 The new empirical model application example

This part presented one case example about the application of the new IRI prediction model for flexible pavement. The case example used mocked data.

The proposed flexible pavement information is presented in Table 13- 7 Pavement structure information Table 13- 7 and Table 13- 8 below. The construction starts from 2022 1st Jan. The problem is to evaluate how IRI varied with time in the following years. According to Table 13- 7 and Table 13- 8, the pavement thickness is 26in (0.66m) and the fine content of the subgrade soil is 14.2. These two values will be used in subsequent calculations.

Table 13- 7 Pavement structure information

Layer number	Layer description	Layer type	Thickness(in)	Layer material
1	Seal Coat	Asphalt concrete layer	0.2	Chip Seal
2	Original Surface Layer	Asphalt concrete layer	3.0	Hot Mixed, Hot Laid AC, Dense Graded
3	Base Layer	Unbound (granular) base	22.8	Crushed Gravel

Table 13- 8 Subgrade soil gradation

Particle size	Average of GT_2MM(>2mm)	Average of COARSE_SAND(2-0.42mm)	Average of FINE_SAND(0.42-0.074mm)	Average of SILT (0.002-0.074mm)	Average of CLAY(0.002mm)
Percentage	29.00	6.50	44.50	14.20	6.10

To evaluate how the IRI varies with time for flexible pavement, the following equation is used:

$$IRI = IRI_0 + IRI_{SF} + 0.292(FC_{Total}) + 0.0038(TC) + 11.28(RD) \quad \textbf{(13- 32)}$$

In Equation (13- 32), IRI_0 is assumed to be 0.5in/mile, which will not change with time; FC_{Total}, TC and RD are the site-measured distress data from 2022 to the following years, which can vary with pavement age. The distress parameter values are not presented here. IRI_{SF} is the site factor induced by climatic effects and pavement properties, it is calculated by:

$$\mathrm{IRI_{sf}} = \mathrm{IRI_{sf_{ref}}} * [\mathrm{age}^{\mathrm{beta}} + 0.0005 * \mathrm{FI_{accum}} * \sin(2\pi * \frac{\mathrm{month}}{12} + 0.35)] \quad \textbf{(13- 33)}$$

In (13- 33), $beta = \frac{0.558}{thickness(ft)} = 0.257$; age is the pavement age start from the construction start year 2022. The variable age can have decimal place to represent different month/season of one year, e.g., 5.5 year means the 5 years plus 6 months of the pavement age; $\mathrm{FI_{accum}}$ is the accumulated monthly freezing index. The value of $\mathrm{FI_{accum}}$ accumulates from July and ends in June of next year. This means $\mathrm{FI_{accum}}$ is always the smallest in July of each year and will be maximum in June of next year for each accumulation period. Example of calculated $\mathrm{FI_{accum}}$ is shown in Table 13- 9 below.

In Equation (13- 33), $\mathrm{IRI_{sf_{ref}}}$ considers the effects of subgrade soil properties on IRI due to site factor, as well as the effects of pavement structure which affects how the IRI developed on the surface of subgrade soil propagates to the surface of pavement structure. It is calculated by:

$$\mathrm{IRI_{sf_{ref}}} = IRI_{sf_{max}} * (-0.188 * ln(0.3048 * thickness(ft)) + 0.131) \quad \textbf{(13- 34)}$$

In Equation (13- 34), the $IRI_{sf_{max}}$ is calculated by:

$$IRI_{sf_{max}} = 0.8 * ln(0.2 * FI + 1) * ln(0.535 * Precip + 1) * ln(0.06 * Silt_{percentage} + 1) \quad \textbf{(13- 35)}$$

In Equation (13- 35), $Precip$ is the average annual precipitation (in) accumulated from January to December of each year; $Silt_{percentage}$ is the percentage of silt content of the subgrade soil; FI is the mean annual freezing index (°F-days) accumulated from January to December of each year. Note that the FI is a constant for each year, whereas the $\mathrm{FI_{accum}}$ in Equation (13- 33) varies with time. Example of $Precip$ and FI were shown in Table 13- 9 below.

The climatic model predicted annual precipitation and temperature data are summarized in Table 13- 9 below. The climatic model predicted monthly temperature can be used to evaluate the freezing index (FI)

of each month from which the accumulated-FI of each month can then be calculated. Example of calculation of the FI_{accum} (from 2022 to 2025) were shown in Table 13- 10 below.

Table 13- 9 Model predicted annual climatic data from 2022 to 2031

Year	Mean annual freezing index (°F-days)	Average annual precipitation (in)
2022	953.2	19.1
2023	906.5	19.1
2024	1110.5	17.4
2025	417.8	18.3
2026	479.8	20.1
2027	780.9	14.9
2028	944.4	20.8
2029	620.8	23.4
2030	909.0	14.6
2031	1038.1	16.8

Based on climatic data in Table 13- 9, using Equation (13- 34) and (13- 35),the $IRI_{sf_{max}}$ and $IRI_{sf_{ref}}$ from 2022 to 2031 were calculated and shown in Table 13- 11. Note that the $IRI_{sf_{ref}}$ is an annual parameter same as annual precipitation and FI.

Put the calculated $IRI_{sf_{ref}}$ into (13- 33), the IRI_{sf} can be calculated when FI_{accum} and age are given. For example, when age is 1.5, according to results of Table 13- 10, the corresponding FI_{accum} should be 1009.2. Then $IRI_{sf} = 6.3 * [1.5^{0.257} + 0.0005 * 1009.2 * \sin(2\pi * 1.5 + 0.04)]$ =6.8 in/mile. Then, the IRI can be predicted using (13- 32): $IRI = 0.5 + 6.8 + 0.1(FC_{Total}) + 0.0009(TC) + 10(RD)$. Following the same procedures, the IRI of different age can be calculated.

Table 13- 10 Example of the calculation of the accumulated-FI (from 2022 to 2025)

Year	Month	Pavement age (Year)	Predicted monthly average T(degC)	Monthly FI(°F-days)	FI_{accum} (°F-days)
2021	7	13.50	16.56	0.00	0.00
2021	8	13.58	19.37	0.00	0.00
2021	9	13.67	10.02	0.00	0.00
2021	10	13.75	7.97	0.00	0.00
2021	11	13.83	4.83	0.00	0.00
2021	12	13.92	-11.31	340.67	340.67
2022	1	14.00	-5.28	177.37	518.04
2022	2	14.08	-11.99	377.47	895.50
2022	3	14.17	-0.46	14.01	909.51
2022	4	14.25	4.08	0.00	909.51
2022	5	14.33	10.72	0.00	909.51
2022	6	14.42	18.95	0.00	909.51
2022	7	14.50	22.23	0.00	0.00
2022	8	14.58	18.16	0.00	0.00
2022	9	14.67	14.21	0.00	0.00
2022	10	14.75	8.67	0.00	0.00
2022	11	14.83	1.53	0.00	0.00
2022	12	14.92	-11.25	337.70	337.70
2023	1	15.00	-10.51	297.77	635.47
2023	2	15.08	-12.92	373.74	1009.20
2023	3	15.17	1.69	0.00	1009.20
2023	4	15.25	8.19	0.00	1009.20
2023	5	15.33	13.42	0.00	1009.20
2023	6	15.42	17.25	0.00	1009.20
2023	7	15.50	21.38	0.00	0.00
2023	8	15.58	17.57	0.00	0.00
2023	9	15.67	14.35	0.00	0.00
2023	10	15.75	5.58	0.00	0.00
2023	11	15.83	-1.07	30.90	30.90
2023	12	15.92	-13.56	408.14	439.04
2024	1	16.00	-9.58	301.15	740.19
2024	2	16.08	-4.09	112.60	852.79
2024	3	16.17	0.42	0.00	852.79
2024	4	16.25	6.50	0.00	852.79
2024	5	16.33	10.71	0.00	852.79
2024	6	16.42	15.84	0.00	852.79
2024	7	16.50	20.35	0.00	0.00

Table 13- 11 The calculated $IRI_{sf_{max}}$ from 2022 to 2031

Year	Mean annual freezing index (°F-days)	Average annual precipitation (in)	Silt content(%)	IRI_sf_max(in/mile)	IRI_sf_ref (in/mile)
2022	953.2	19.1	14.2	21.85	6.4
2023	906.5	19.1	14.2	25.43	6.3
2024	1110.5	17.4	14.2	24.97	6.2
2025	417.8	18.3	14.2	21.01	5.4
2026	479.8	20.1	14.2	23.02	5.9
2027	780.9	14.9	14.2	21.00	5.3
2028	944.4	20.8	14.2	27.10	6.7
2029	620.8	23.4	14.2	26.75	6.7
2030	909.0	14.6	14.2	21.32	5.4
2031	1038.1	16.8	14.2	24.01	6.0

13.9 The inputs of three levels of the empirical models

Like the simplified 1-D model as presented in Appendix 6, the empirical IRI models can also have different levels of design based on input conditions. The input of the three levels of the empirical IRI model is presented in Table 13- 12 below.

Table 13- 12 The Inputs of three levels of the empirical models

Input types	Level 1	Level 2	Level 3
Asphalt concrete (AC) surface model			
Climatic inputs			
Annual FI (degF day)	x(no need)	√	√
Historical monthly Accumulated FI (degF day)	√	√	√
Annual Precipitation	x	√	√
Pavement information			
Layer thickness	x(no need)	√	√
Age	√	√	√
Historical IRI variation with time	√	√	x(no need)
Subgrade silt content	x(no need)	√	√
Calibrated coefficients			
IRI_sf_ref	√	x (Correlation equation)	x (Correlation equation)
beta	√	x (Correlation equation)	x (Correlation equation)
gama	x(no need)	√	x (default)
eta	x(no need)	√	x (default)
e1-e4	x(no need)	√	x (default)
HMA overlay model			
Climatic inputs			
Annual FI (degF day)	x(no need)	√	√
Annual Precipitation	x	√	√
Pavement information			
thickness_AC (asphalt thickness)	x(no need)	√	√
L_0	x(no need)	√	√
Age	√	√	√
Age_inc	√	√	x (Correlation equation)
t_overlay	x(no need)	x(no need)	√

Historical IRI variation with time	√	√	x(no need)
Subgrade silt content	x(no need)	√	√
Calibrated coefficients			
IRI_sf_ref	√	x (Correlation equation)	x (Correlation equation)
beta	√	x (Correlation equation)	x (Correlation equation)
e2-e4	x(no need)	√	x (default)
Continuously reinforced concrete pavement (CRCP) model			
Climatic inputs			
Annual FI (degF day)	x(no need)	√	√
Annual Precipitation	x	√	√
Pavement information			
L_b	x(no need)	x(no need)	√
L_c	x(no need)	x(no need)	√
Thickness (total thickness)	x(no need)	√	√
Age	√	√	√
Age_inc	√	√	x (Correlation equation)
Historical IRI variation with time	√	√	x(no need)
Subgrade silt content	x(no need)	√	√
Calibrated coefficients			
IRI_sf_ref	√	x (Correlation equation)	x (Correlation equation)
beta	√	x (Correlation equation)	x (Correlation equation)
e2-e4	x(no need)	√	x (default)

13.9.1 The flexible pavement IRI model design level

As discussed above, the proposed flexible pavement IRI models are:

$$IRI = IRI_0 + IRI_{SF} + c_1(FC_{Total}) + c_2(TC) + c_3(RD) \quad \textbf{(13- 36)}$$

$$\mathrm{IRI_{sf}} = \mathrm{IRI_{sf_{ref}}} * [\mathrm{age^{beta}} + \mathrm{gama} * \mathrm{FI_{accum}} * \sin(2\pi * \mathrm{age} + \mathrm{eta})] \quad \textbf{(13- 37)}$$

The level 1 design needs already known and constant $\mathrm{IRI_{sf_{ref}}}$ and beata. All other coefficients in Equation (13- 36) and (13- 37) need to be regressed based on historical IRI data, in essence, it is pure regression. Level 1 analysis is suitable for sections that already have historical IRI data, not suitable for new pavement design, but suitable for an existed pavement with historical monitoring data. The level 2 design assumes $\mathrm{IRI_{sf_{ref}}}$ will change from year to year and is evaluated using below correlation equations:

$$\mathrm{IRI}_{sf_{ref}} = \mathrm{IRI_{sf_{max}}} * DF_T \quad \textbf{(13- 38)}$$

$$DF_T = -0.188 * ln(0.305 * thickness(ft)) + 0.131 \quad \textbf{(13- 39)}$$

$$IRI_{sf_{max}} = e_1 * ln(e_2 * FI + 1) * ln(e_3 * Precip + 1) * ln(e_4 * Silt_{percentage} + 1) \quad \textbf{(13- 40)}$$

For level 2 design, the coefficients gama, eta, and e1 to e4 in Equation (13- 37) and (13- 40) needs calibration (obtained by regression) using historical measured IRI data. Level 2 analysis is suitable for sections already have historical IRI data, not suitable for a new pavement design. In addition, the coefficient beta is calculated using correlation equations in the level 2 design:

$$beta = \frac{0.558}{thickness(ft)} \quad \textbf{(13- 41)}$$

For level 3 design, Equations (13- 7) to (13- 10) is used to evaluate IRI, where all the coefficients are calibrated as presented in 13.4. The level 3 analysis is suitable for sections of a new pavement design when future climatic data and distress conditions can be forecasted.

13.9.2 The HMA overlay IRI model design level

As discussed above, the proposed HMA overlay pavement IRI models are:

$$IRI = IRI_0 + IRI_{SF} + c_1(FC_{Total}) + c_2(TC) + c_3(RD) \quad \textbf{(13- 42)}$$

$$\mathrm{IRI_{sf}} = \begin{cases} 0 & when\ (age < age_{inc}) \\ \mathrm{IRI_{sf_{ref}}} * (age - age_{inc})^{beta} & when\ (age > age_{inc}) \end{cases} \quad \textbf{(13- 43)}$$

$$\mathrm{IRI}_{sf_{ref}} = \mathrm{IRI_{sf_{max}}} * DF_T \quad \textbf{(13- 44)}$$

For level 1 analysis, the historical IRI data (or model predicted IRI data) is required, from which age_{inc} can be obtained. Like the level 1 design of flexible pavement IRI models, the HMA overlay models also need $\mathrm{IRI_{sf_{ref}}}$ and beata are constant and known, but all other unknown parameters need to be calibrated via historical IRI data. In essence, this process is a pure regression process. The level 1 analysis is suitable for sections already have historical IRI data, not suitable for a new pavement design.

The level 2 analysis also needs historical IRI and age_{inc}. In addition, level 2 analysis assumes $\mathrm{IRI_{sf_{ref}}}$ changes from year to year and is evaluated using correlation equations:

$$\mathrm{IRI}_{sf_{ref}} = \mathrm{IRI_{sf_{max}}} * DF_T \quad \textbf{(13- 45)}$$

$$DF_T = 0.1517 * \exp(-0.82 * L_0) \quad \textbf{(13- 46)}$$

$$\mathrm{IRI_{sf_{max}}} = \ln(\mathrm{e_2FI} + 1) * \ln(\mathrm{e_3Precip} + 1) * \ln\left(\mathrm{e_4Silt_{percentage}} + 1\right) \quad \textbf{(13- 47)}$$

where coefficients e2 to e4 are obtained by regression using historical IRI data. The coefficient beta is evaluated using correlation equations.

$$beta = 0.206 * thickness_{AC}^{-1.62} \quad \textbf{(13- 48)}$$

For level 3 design, Equations (13- 23) to (13- 26) is used to evaluate IRI, where all the coefficients are calibrated as presented in 13.6. The level 3 analysis is suitable for sections of a new pavement design when future climatic data and distress conditions can be forecasted.

13.9.3 The CRCP pavement IRI model design level

As discussed above, the proposed CRCP pavement IRI models are:

$$\mathrm{IRI_{sf}} = \begin{cases} 0 & when\ (age < age_{inc}) \\ \mathrm{IRI_{sf_{ref}}} * (age - age_{inc})^{beta} & when\ (age > age_{inc}) \end{cases} \quad \textbf{(13- 49)}$$

$$\mathrm{IRI_{sf_{ref}}} = ln(0.01FI + 1) * ln(0.0165Precip + 1) * ln\left(9.9Silt_{percentage} + 1\right) \quad \textbf{(13- 50)}$$

The level 1 analysis requires historical IRI data because the age_{inc} can only be obtained from the historical IRI vs. time. Like the flexible pavement and HMA overlay models, the level 1 design for CRCP model get most unknown parameters in Equation (13- 49) and (13- 50) through regression except for $\mathrm{IRI_{sf_{ref}}}$ and beata which are user provided and set as constant. Apparently, the level 1 analysis is suitable for sections that already have historical IRI data, not suitable for a new pavement design.

The level 2 analysis also needs historical IRI data to get age_{inc}. The level 2 analysis assumes $\mathrm{IRI}_{\mathrm{sf}_{\mathrm{ref}}}$ change from year to year and is evaluated using correlation equations:

$$\mathrm{IRI}_{\mathrm{sf}_{\mathrm{ref}}} = ln(e_2 FI + 1) * ln(e_3 Precip + 1) * ln\left(e_4 Silt_{percentage} + 1\right) \quad \textbf{(13- 51)}$$

where coefficients e2 to e4 can be regressed using historical IRI data. The coefficient beta is estimated using correlation equations:

$$beta = 0.01 \exp(-0.61 * thichness) \quad \textbf{(13- 52)}$$

The level 3 analysis compute IRI using Equation (13- 29) to (13- 31) and the level 3 analysis is suitable for sections of a new pavement design.

13.10 References

Yoder, E. J., and Witczak, M. W. (1975). "Principles of pavement design." Second Ed., John Wiley and Sons, New York, N.Y.